Addis Ababa University

Collage of Technology and Built Environment (CTBE)

School of Electrical and Computer Engineering

Sliding Mode Based Maximum Torque per Ampere and wide speed range Control for Interior Permanent Magnet Synchronous Motor Drive

A Thesis submitted to Addis Ababa Institute of Technology, School of Graduate Studies, Addis Ababa University

In partial fulfilment of the requirement for the Degree of Master of Science in Electrical and computer Engineering (Electrical Control Engineering).

By:

Netsanet Abate

Advisor: - Dr. Mengesha Mamo, Associate Professor (PhD)

ADDIS ABABA ETHIOPIA

June, 2025

Addis Ababa University

Collage of Technology and Built Environment (CTBE)

School of Electrical and Computer Engineering

“Sliding Mode Based Maximum Torque per Ampere and wide speed range Control for Interior Permanent Magnet Synchronous Motor Drive”

By: Netsanet Abate

Approval by Board of Examine

Dr. Sosina Mengistu (PhD)	-
School Head	Signature
Dr. Mengesha Mamo, Associate Professor (PhD)	-
Advisor’s Name	Advisor Signature
Dr. Mesifin Tilahun (PhD)	-
Internal Examiner	Signature
Dr. Lebesewerik Negash, Assistant Professor (PhD)	-
External Examiner	Signature

Declaration

I, the undersigned, Netsanet Abate declare that this thesis work expect reference to other people's work and which have been duly listed was the result of my own original work and that it has neither in part nor in whole be presented for the Award of Masters of Science Degree or Certificate in the Addis Ababa University Institute of Technology winnable or elsewhere.

Author Signature

Netsanet Abate _____

Place:

Addis Ababa Institute of Technology, AAiT

Addis Ababa University, AAU

Addis Ababa, Ethiopia.

Submitted by: June 19, 2025.

This thesis has been submitted for examination with my approval under university advisor Dr. Mengesha Mamo, Associate Professor (PhD).

Dedication

This Thesis Work is Dedicated for my Family especially My father Abate Astatikie & Mother Eshetua Tura.

To my parents, whose sacrifices and guidance have shaped who I am today; to my siblings, who have always been there with a listening ear and a word of inspiration; and to my whole family, whose love and support have been my greatest inspiration.

Thank you for being my rock and my greatest cheerleaders.

With all my love and gratefulness,

Netsanet Abate

Acknowledgment

I want to express my profound gratitude to Dr. Mengesha Mamo, Associate Professor (PhD), who served as my thesis advisor, for his unwavering encouragement, support, and direction throughout my research. His support and participation enabled me to complete this thesis. Additionally, I want to thank my thesis committee, which consists of Getinet (MSc), Nebiyu Tenaye (PhD candidates), and Dr. Libsework Negash, Assistant Professor (PhD), for their assistance.

I also like to express my gratitude to my close friends and research peers. Above all, I want to thank my parents and friends from the bottom of my heart for their support.

Abstract

This thesis presented an Interior Permanent Magnet Synchronous Motor (IPMSM) drive system with a sliding mode-based Maximum Torque per Ampere (MTPA) and wide-speed range (field weakening) control. It developed and analysed an IPMSM motor dynamic model, empowering motor control in both constant-torque (constant flux) and wide-speed range (constant-voltage-ampere) modes. The control performance of the IPMSM varied due to temperature changes and magnetic saturation, so a sliding mode-based MTPA controller with a First-Order Sliding Mode Controller (SMC) was used to address model uncertainty and external disturbances. The scheme eliminated steady-state error using an Integral Sliding Mode Controller (I_SMC). MATLAB simulations were performed to validate the proposed controller.

Keyword's: - Interior permanent magnet Synchronous Motor (IPMSM), Maximum Torque Per Ampere (MTPA), Wide speed range control, Field Weakening (FW), Sliding Mode Controller (SMC).

Table of Contents

List of Figure

List of Tables

List of Symbols and Abbreviation

IPMSM	Interior Permanent Magnet Synchronous Motor
SMC	Sliding Mode Control
I-SMC	Integral Sliding Mode Control
WSRC	Wide Speed Range Control
PMSM	Permanent Magnet Synchronous Motor
AC	Alternating Current
DC	Direct Current
FOC	Field Oriented Control
FW	Field Weakening
HVDC	High Voltage Direct Current
EMF	Electromotive Force
SVM	Space Vector Modulation
SVPWM	Space Vector Pulse Width Modulation
SPWM	Sinusoidal Pulse Width Modulation
PI	Proportional Integral
SM	Synchronous Machine
MTPA	Maximum Torque per Ampere
PWM	Pulse Width Modulation
VSI	Voltage Source Inverter
TF	Transfer Function
THD	Total Harmonic Distortion

2D	Two Dimension
3D	Three Dimension
id , iq	d and q stator currents
ua, ub , uc	stator phase voltages
Rs	stator resistance
Usd , Usq	d and q components of the stator voltage vector
fsw	switching and sampling frequency
e	Error
τ	Time Constant
Ω	Ohm
ω	Speed
θ	Rotor Position angle theta
λpm	Permanent Magnet Flux Linkage
J	Inertia, Performance Index
B	Viscous Friction Dumping Constant, Performance Index
Ts	Sampling Time
K	Gain
L	Inductance
U	Voltage
I	Current
T	Torque
p	Power

P	Number of Poles pair
EF	Electromotive Force
BEF	Back Electromotive Force

Chapter One

1. Introduction

1.1 Background

Among the frequent appealing features of IPMSMs are their high torque-to-inertia ratio, high power density, and broad speed operating range. IPMSMs have therefore been used in numerous industrial applications [1]. However, the control typical of IPMSMs tends to time-varying performance due to the machine parameters difference caused by the magnetic saturation [2]. For the IPMSM, the quadrature-axis inductance is increased by the rotor magnetic circuit saliency, which leads to a reluctance torque term including into the torque equation [3]. However, to use the advantage of the reluctance torque term in the constant torque and flux weakening area, appropriate control methods are required. Therefore, the method of using the high-frequency variation of the output sliding mode controller obtains the advance angle of stability of the MTPA for an IPMSM is proposed. Moreover, the method proposing in [4] uses the built-in feature of the MTPA operation to create the d-axis current command and track the MTPA operating point by injecting a tiny virtual current angle signal [5]. With model-based torque improvement in [6], a strong torque response and exact and effective torque control. Flied Weakening control can be accomplished in a number of ways, including current control, voltage control and flux control in [2]. Robust nonlinear control technique to achieve a wide-speed-range operation of the IPMSM based on the MTPA and Field Weakening (FW) controls was offered [7]. a strong torque response and exact and effective torque control. Feld Weakening control can be accomplished in a number of ways, including current control [8].

Moreover, a sliding mode-based design method of a voltage phase controller for the IPMSM was presented in [8]- [9]. The voltage phase controller controls the torque only in a high-speed region where the inverter output voltage amplitude is saturated. Furthermore, in [10]- [11], a voltage feedback FW control scheme for vector-controlled IPMSM drive systems is considering. A voltage control loop is also designed in this study to limit the inverter output voltage to the maximum output voltage of the inverter at high-speed for the FW control.

1.2 Statement of The Problem

The dynamic performance of an IPMSM is characterized by high nonlinearity, joined with losses such as copper and hysteresis losses in the stator. In topical studies referenced in modern theses, Sliding Mode Control (SMC) has garnered important care due to its strong robustness and fast response in the face of time-varying uncertainties, including variations in internal parameters and external disturbances [12]. However, a well-known disadvantage of SMC is the occurrence of chattering caused by the switching mechanism [13]. To lessen this issue, strategies such as the first-order SMC have been employed. This approach not only reduces chattering but also offers reliable control precision. Though, that the design of first-order SMC typically requires prior knowledge of the bounds of uncertainties, which can be difficult to determine in real-world applications [4]. As a result, various nonlinear control strategies integrating adaptive or intelligent control techniques have been developed to estimate these uncertainties in IPMSM systems. [3], [14].

Research on SMC approaches that consider the impact of the IPMSM's reluctance torque is, nevertheless, extremely rare [15]. This thesis proposes an SMC speed controller that takes nonzero d-axis current into consideration in order to enhance the robust control performance of the IPMSM drive system under parameter variations and external disturbances. [17]. A good performance IPMSM drive system with sliding mode based MTPA and FW control is proposing in this Thesis. May be if it has a chattering phenomenon second order sliding mode controller is applying to eliminate chattering to Integral sliding mode is applied if there is a study stat error [16]. Lyapunov stability theorem is used to derive the ambiguity to ensure that the sliding mode speed controller is asymptotically stable. The study includes theories and modelling of the MTPA and FW controls of the IPMSM drive are presenting, the sliding mode speed controller will be developing, to confirm the exactness and robustness of the proposing best-performance control methods. At the end the expected result is verified with simulation in MATLAB Simulink.

1.3 Objectives of The Study

General Objective

The general objective of this proposal is to obtain a detailed dynamic model of MTPA control that describes the IPMSM and to design sliding mode controller for a chattering free sliding mode controller to control the maximum torque controller and wide speed range

Specific Objective

- To develop a detailed nonlinear dynamic model that describes the IPMSM.
- To implement the nonlinearity of MTPA control.
- To design a chattering free sliding mode controller for the IPMSM.
- To develop simulation for the designed sliding mode controller using
- MATLAB Simulink

1.4 Contribution of The Thesis Work

Using Interior Permanent Magnet Synchronous Motors (IPMSMs) for Maximum Torque per Ampere (MTPA) control and wide-speed-range operation with Sliding Mode Control (SMC) is an effective approach in applications requiring high efficiency and performance, particularly in electric vehicles and industrial drives. Here are some key contributions and insights on this topic.

- The dq_axis model reference frame is employed and arranges the necessary rule in rotating magnetic field modeling on IPMSM.
- The saliency of IPMSM is used, which requires analyzing the high frequency component of the stator current. From which the inductance of the rotor can be obtained and, hence, the rotor angle.
- This thesis used MTPA Control Strategy that has an Objective of Optimized torque production while minimizing current draw and they can Implemented Calculation that can optimal rotor flux linkage and current references for varying speeds, enabling maximum torque output per unit of current.
- Wide Speed Range Operation is used on this thesis to Decoupling the current control Used vector control to decouple torque and flux control, facilitating efficient operation across a wide speed range.

- This thesis implements a Sliding Mode Control (SMC) strategy for nonlinear control by designing a sliding surface that guides system trajectories to desired dynamics. To correct steady-state errors, Integral Sliding Mode Control (ISMC) is employed. SMC offers robustness against parameter variations and disturbances, effectively handling uncertainty in IPMSM applications. It enables rapid response to load torque and speed changes, critical for high-performance systems, while minimizing energy loss by operating the motor at its optimal point. However, SMC faces challenges such as chattering, which may cause mechanical wear. To address this, advanced techniques like ISMC, higher-order SMC, and smooth approximations are being explored. Accurate IPMSM models are developed to simulate MTPA under varying torque conditions, and experiments validate the SMC approach for stability and efficiency in speed and torque tracking.

1.5 Methodology

In order to accomplish this thesis with a best controlled output. Initially a detailed dynamic model of the IPMSM has to be determined. In this proposal fully utilize the IPMSM reluctance torque it means that in their control scheme the stator q-axis current is proposed to the torque command. By this assertion it is quite straight forward to achieve a linear torque control for IPMSM drive in addition in designing the related nonlinear slid mode controllers they did not take in to account all possible IPMSM drive nonlinearities due to uncertainties.

According to the proposing scheme presented in this work sliding mode controller is introducing which is capable of conserving the system the system robustness and stability against all parameter variation and external load torque disturbance. In this design in order to make number of parameter estimation minimal a procedure design is using that possess strong stability properties that through those using over parameterization. Using the Lyapunov stability theory, the controller and parameter estimation low are developed first then is show that under system wide speed range condition the estimation error in motor d-q axis inductance as well as estimated error in the rotor flux linkages asymptotically tend to zero.

In the control scheme reference of d-q axis currents generate on the bases of MTPA control and wide Speed Range control scheme relating to the IPMSM drive. In addition, the conventional speed SMC controller generates the torque reference signal.

The performance of the propose sliding mode controller nonlinear control scheme is verifying by simulation. It Implemented according to the following steps.

- **Mathematical Modelling**: - Derive the mathematical model of the IPMSM, including voltage, current, and torque equations.
- **Control Law Development**: - Define the sliding surface and establish the control law based on Lyapunov stability criteria to ensure the system remains on the sliding surface. And integral sliding mode control to control study state error
- **Implementation:** - Use MATLAB 2022b simulation digital and expect to apply on real-time implementation of the SMC algorithm, incorporate sensors for feedback, including current and rotor position sensors.
- **Tuning and Optimization**: - Tune the control parameters for PI current controller and apply the sliding mode controller to achieve optimal performance under varying conditions.
- **Performance Evaluation:** - Conduct a thorough evaluation of system performance through simulations on MATLAB 2022b and focused on efficiency, dynamic response, and robustness.

1.6 Scope and Limitation

The scope of this thesis is developing Simulink model on MAT-lab for the simulation to verify that MTPA and wide speed range speed control result is achieved. Thus, it implies that the thesis doesn't include practical hardware implementation.

1.7 Outline of The Thesis

This thesis contains six chapters and each chapter focuses on different particulars of the sensored IPMSM drive. Chapter-1 presents the background and problem description of IPMM drive system, and the objectives and involvement of the thesis.

Chapter-2 includes construction of interior permanent magnet synchronous motor with their type, Interior Permanent Magnet Synchronous Motor rotor topologies and literatures review. Also, it includes presents the concepts of park Clarke transformation $dq-axis$, the dynamic mathematical modelling equation to drive the instantaneous current and voltage output of IPMSM and mathematical model verifications and its simulation.

Chapter-3 presents topology of vector field oriented control, maximum torque per ampere controller strategy and wide speed range controller strategy, concepts and working principle on SVPWM technique and power invertor.

Chapter-4 includes Sliding mode controller (SMC) definition and their type is presented also implementation of SMC designed also apply Lyapunov stability implemented. The current controller is applied by using tuning of the PI. The speed and torque performance in both commands of the drive system next to the corresponding performance variables, currents and voltages, are also accessible and investigated in this chapter includes the simulation result is presented.

Chapter-5 from the thesis trainings, conclusions, recommendations and future works are presented.

Chapter Two

2 Literature Review and IPMSM Model Verification

2.1 Introduction

Electric motors for traction applications require high torque and power density, and wide speed range with high efficiency. Permanent Magnet Synchronous Motors (PMSMs) have become prevalent in recent years and are commonly used in industrial automation, robotics, and aerospace. This is due to their high-power capability that has higher efficiency and higher torque density compared to induction and synchronous reluctance machines. Comes with lower mass and moment of inertia. As a permanent magnet is used to generate rotor flux, there are no losses in a rotor and this makes this type the most efficient among all AC machines [1].

2.2 Construction of IPMSM

PMSMs are two type of construction according to permanent magnet mounted position on the rotor of PMSM

1. Surface Mounted Permanent Magnet Synchronous Motor (SPMSM) and
2. Interior Permanent Magnet Synchronous Motor (IPMSM).

PMSM are three phase motor connected with an AC supply. These windings are distributed in a sinusoidal manner separated by the phase shift of 120^0. It helps to avoid the harmonic components of a higher order PMSM types and also enables the machine to generate the air-gap field that typically contains the fundamental sinusoidal component. As synchronous motors are doubly-excited system (a magnetic system that uses two independent coils to produce a magnetic field.), the other foundation of excitation, PM in the rotor an important role in the development of these machines. The stator and rotor magnetic fields continue in synchronised with each other. Therefore, this kind of the drives are preferred in constant speed applications.

2.3 Interior Permanent Magnet Synchronous Motor rotor construction

On IPMSM Because of their prominent nature, they are typically chosen for high-speed applications. In these machines, the permanent magnets are hidden within the rotor core. In general, IPMSM can be divided into three types: axial flux, transversal

flux, and radial flux machines, depending on the flux that passes through its air gap[18]. Directing on the placement of PMs inside the rotor surface, the main classes of IPMSM are given

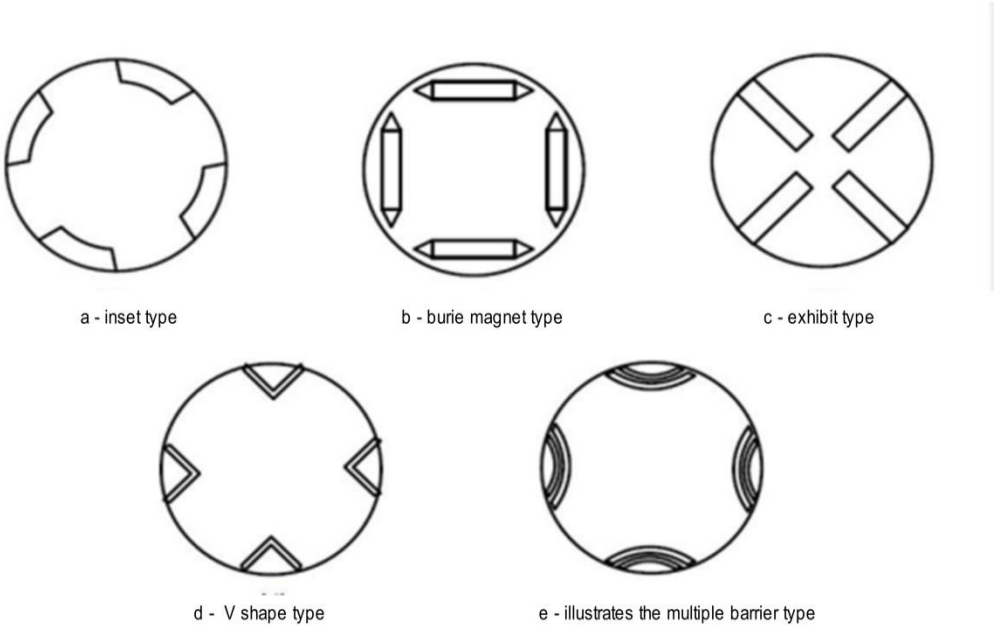

Figure 2-2: Interior Permanent Magnet Synchronous Motor rotor type

This figure shows that the placement of Permanent Magnet in IPMSM [19] Very small iron bridges are provided at the end of magnet poles in the IPMSM that usually saturate because of the leakage flux. The flux barriers between these iron bridges and magnetic poles are made of non-magnetic materials to avoid short circuit with the adjacent magnetic poles.

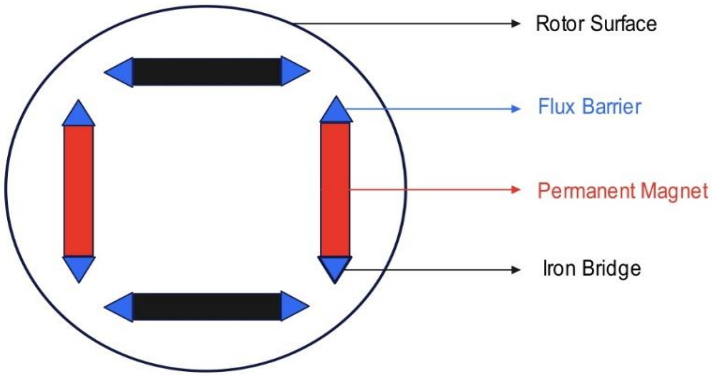

Figure 2-3: placement of Permanent Magnet in IPMSM

Saliency (ξ)

Saliency(ξ) is the characteristic of PMSM, that affect significantly on the wide speed range properties. A maximum speed achievable in these machines depends on saliency ratio as well.

The concept of the saliency ratio arises from the distinction between the direct-axis and quadrature-axis inductances, $\boldsymbol{L_d}$ and $\boldsymbol{L_q}$. This ratio, often denoted as $\boldsymbol{\xi}$, reflects the comparative values of these two inductances. In Surface Permanent Magnet (SPM) motors, this saliency is minimal or non-existent because $\boldsymbol{L_d}$ and $\boldsymbol{L_q}$ are almost equal. On the other hand, Synchronous Reluctance Machines (SyRMs) exhibit high saliency ratios due to their reliance on reluctance torque, with no contribution from permanent magnet (PM) flux.

$$\boldsymbol{\xi = \frac{L_q}{L_d}} \qquad 2.1$$

Interior Permanent Magnet Synchronous Motors (IPMSMs) are typically engineered to have saliency ratios in the range of 2 to 3. Nonetheless, machines with either extremely low or very high saliency ratios face limitations in achieving high speeds across broad speed ranges. A motor with a low saliency ratio—around 1.05, for instance—struggles to express its saliency-based characteristics effectively in terms of torque and speed. As illustrated, when saliency is weak or absent, the machine's efficiency in producing torque and power diminishes significantly.

The DTC method addresses drawbacks of the previously stated method as there is no need for current controller, which results in elimination of time delay caused by a current loop; and more importantly, knowing rotor position is not required anymore, which means no encoder and uncertainties associated with it [1] . Despite the advantages mentioned above, it has disadvantages when compared to FOC. The use of hysteresis controllers to choose the appropriate voltage vector is what causes the high ripples. [1]. Additional inverters must be added in order to overcome it, or lessen ripples, which raises the cost and complicates implementation. [7]. But because rare-earth magnets are in high demand and their price fluctuates a lot, research is currently focused on designing alternative electric machine technologies that either don't utilize rare-earth magnets or use less of them.

Permanent Magnet Minimization

The load performance and reliable output of the IPMSM are determined by the prudent use of PMs. Reducing the PMs' cross-sectional area is another efficient

method to increase their usage rate and lower the cost of the efficient materials. The air gap flux and the air gap magnetic field waveform that the PM motor requires mostly dictate the width of PMs. [22]. The impact of PM thickness on the air gap magnetic field's magnetic flux density amplitude is less significant than that of PM width on the air gap magnetic field. The PM motor's operating point primarily dictates the choice of PM thickness, which is intimately tied to the d-axis inductance. Therefore, the relationship between the motor characteristic current, PM flux, and the d-axis inductance is stated in Equation in order to make better use of PMs and achieve the highest power output of IPMSM in a wide speed regulation range. [20].

$$i_{ch} \geq i_{max} = \frac{\lambda_{pm}}{Ld} \qquad 2.2$$

where, i_{ch}- the characteristic current and i_{max}-the stator rated current amplitude in the dq coordinate system, λ_{pm} is the excitation flux linkage of the Permanent Magnet.

Scalar Control

Scalar control is the simplest way to manage an IPMSM, primarily focusing on the magnitude of voltage or current and maintaining a consistent ratio with frequency as the motor's speed changes. This open-loop method operates without motor feedback, making it easy and inexpensive to implement. However, this simplicity brings downsides: poor dynamic performance and instability at higher frequencies. To counteract instability, rotors often need damper windings for synchronization, a feature most PMSMs lack. Consequently, scalar control is best suited for less demanding applications, such as fans or pumps

Vector Control

Initially, vector control was the go-to for high-performance applications – places where smooth speed changes and robust low-speed torque were non-negotiable. Think robotics, electric vehicles, or industrial machinery. But here's the exciting part: thanks to rapid advancements in computing power and more affordable electronics, FOC is no longer just for the top-tier systems. It's rapidly becoming viable for simpler applications too. Why? Because it offers remarkable efficiency gains in terms of motor size, overall system cost, and, crucially, energy consumption. Many experts predict that as computing power continues its impressive march forward, vector control is poised to replace traditional scalar control methods across a much wider

range of applications, becoming the new standard for efficient and precise motor management.

2.4 Literature Review

One significant advantage of an internal permanent magnet (IPM) motor lies in its rotor design, where the permanent magnets are embedded rather than mounted on the surface. This strategic placement allows the motor to harness reluctance torque, boosting its overall performance. Furthermore, embedding the magnets substantially reduces the likelihood of them breaking loose due to the powerful centrifugal forces experienced during high-speed operation, a common concern with surface permanent magnet (SPM) designs. The author in reference [1] High efficiency, high power density, high torque-to-inertia ratio, wide speed operation range, and low maintenance costs are just a few of the many alluring features that have made IPMSMs so popular. Despite the fact that there are numerous vector controls for variable speed applications of IPMSMs in the literature, they may generally be divided into two categories: linear torque control method and nonlinear torque control strategy. IPMSM's fundamental mathematical modeling, which might be applied to the creation of appropriate stabilizing control techniques.

Authors in reference [2] present demonstrated that the dynamic model of the IPMSM is linearized by sliding mode controller theory and then a linear controller is designed to control the rotation of the linearized dynamic model of the IPMSM also to control the MTPA and field weakening is including in the model

Authors in reference [3] a detail mathematical model for IPMSM drive MTPA and over full speed control. The nonlinearity dynamic model of IPMSM formulating using Newton’s method low and the field weakening is also designed and modelled detailed

Authors in reference [4] present, we spent a large amount of time and energy determining the direct-axis reference current equations. Two sophisticated control strategies depend on these equations of Maximum Torque Per Ampere (MTPA): This maximizes efficiency by obtaining the maximum torque from each ampere of current. Achieving the maximum power output for the specified current input is the goal of the Maximum Power Per Ampere (MPPA) method. We also presented the ideas of a Sliding Mode Controller in addition to these fundamental equations. After that, we outlined every equation needed to truly create and put into use this reliable controller.

Authors in reference [15] proposed the IPMSM drive by identifying the rotor's initial position. A high frequency signal is injected to detect the position of the rotor from rotor's magnetic saliency. This Thesis uses the same approach as the Thesis in [Novel Rotor Position Extraction Based on Carrier Frequency Component Method (CFCM) Using Two Reference Frames for IPMSM Drives], except that this Thesis presents performance of the drive system. According to this Thesis, an IPMS motor makes the magnetic and reluctance torque simultaneously and the high torque per current can be generated. To obtain the high reluctance torque and to hold high efficiency.

Authors in reference [16] is proposed for salient-pole permanent magnet synchronous motor (PMSM), the amplitude of extended back electromotive force (EEMF) is determined by rotor speed, stator current and its derivative value also proposes a novel position sensor less control strategy for PMSM considering saliency. On this Thesis they bullet a novel full-order SMO is built to estimate the rotor position. The effectiveness of the proposed method is validated on a low voltage salient-pole PMSM, but they are not work on MTPA control and field weakening strategies.

Authors in reference [3] is Proposed Controlling electric motors at high speeds can be challenging due to small electrical angle delays, often caused by inverter issues or design flaws. These delays lead to rotor position errors that worsen with speed. To address this, engineers use two main detection approaches:

Initial rotor position detection assumes a fixed delay, making it less reliable at higher speeds.

Time-delay position detection, the focus of this study, accurately detects and compensates for varying delays, improving torque control and motor performance despite hardware inconsistencies.

Authors in reference [21] With an emphasis on flux-weakening techniques that offer maximum torque per ampere (MTPA) and maximum torque per volt (MTPV), this research study employs a novel approach to regulate the speed and torque of internal permanent magnet synchronous motor drives. The efficiency and performance of the motor have been enhanced by the suggested controller. Field weakening was employed in MTPA to improve the higher speed range. Additionally, the full speed range is displayed using the MTPV approach. In order to minimize losses, the suggested controller set a limit on the current value. And they conclude FW is to limit the reduction in torque when the motor is running at higher speeds than the rated

speed. If the MTPA control system was not used. For the same torque, the motor currents increased, which led to higher stator losses. It is interesting to see the impact that MTPA algorithm has on the performance and efficiency of the engine. FW was used with MTPA to achieve better higher speed range. Also, the MTPV method is used to display the entire speed range. Stator losses have reduced significantly, motor performance has improved and the total available torque has not decreased that much in the FW range.

Authors in reference [8] By guaranteeing system stability from the beginning and resolving instability during the SMC's initial reaching phase, Integral Sliding Mode Control (I-SMC) improves traditional Sliding Mode Control (SMC). I-SMC combines discontinuous control to manage disturbances with nominal control for optimal conditions. We used a disturbance observer in conjunction with I-SMC on a surface-mounted PMSM in our investigation. By anticipating changes in load, the observer enables the controller to maintain precise speed tracking and reliable operation. This strategy provided better resistance to parameter changes and outside disturbances than PI and simple SMC techniques.

Model Predictive Control (MPC) and Super Twisted Sliding Mode Control (ST-SMC) are two advanced control techniques widely utilized in the operation of Permanent Magnet Synchronous Motors (PMSMs). This review focuses on Maximum Torque Per Ampere (MTPA) strategies and wide speed control implementations, particularly leveraging ST-SMC.MTPA Strategy aims to optimize motor performance by maximizing torque output for a given current input. This approach is critical in applications where efficiency and performance are paramount, such as electric vehicles and industrial drives. The MTPA Principles strategy involves the calculation of optimal current vectors to ensure the motor operates at maximum efficiency. Researchers have developed algorithms that compute these vectors in real-time, enhancing performance under varying load conditions. One of the significant challenges in implementing MTPA is the real-time computation of optimal currents, particularly in wide speed ranges. Traditional methods may not suffice, especially under dynamic operational conditions. Wide speed control encompasses a range of control strategies that maintain performance across various speeds. There are several techniques employed for wide speed control, including scalar control, vector control, and direct torque control. Each method has its advantages and limitations in terms of

response time, complexity, and efficiency. The effective of wide speed control should focus on torque ripple, dynamic response, and robustness against disturbances.

Super Twisted Sliding Mode Control (ST-SMC) offers a robust alternative for controlling PMSMs, particularly in the presence of uncertainties and disturbances. The features of the ST-SMC is characterized by its ability to provide finite-time convergence and chattering reduction, making it suitable for high-performance applications. It operates by enforcing a sliding condition on the system dynamics, allowing for robust tracking of desired trajectories. Advantages Compared to traditional sliding mode controllers, ST-SMC improves robustness and reduces the effect of parameter variations, which is essential for applications with high variability.

Integration of MTPA and ST-SMC Recent studies have explored the integration of MTPA strategies with ST-SMC to enhance the overall performance of PMSMs. The Control Architecture proposed architecture typically involves a two-layer control structure where the outer layer determines the MTPA current references, and the inner layer implements ST-SMC to track these references. Implementations have shown improved torque output, reduced energy consumption, and enhanced robustness against parameter variations. The combination allows for effective control over a wide speed range while maintaining efficiency. At the last there conclusion is the integration of MTPA with Super Twisted Sliding Mode Control presents a promising avenue for improving the performance of PMSMs across a wide speed range. While challenges remain, ongoing research continues to refine these techniques, aiming for enhanced robustness and efficiency in real-time applications.

2.5 The IPMSM Mathematical and model verification simulation

IPMSMs' small size, high efficiency, and power density make them popular in high-performance industries like electric automobiles. Motors in EVs have to maintain exact speed in spite of obstacles including shifting parameters, load variations, and inaccurate models. Accurate modeling is challenging because to these disturbances, which include friction and current coupling. Because of this, traditional control strategies frequently fail, necessitating the use of sophisticated control strategies for reliable and effective motor operation.

Under basic Mathematical modelling of IPMSMs involves establishing equations that describe their electrical and mechanical dynamics. Here's a basic outline of the modelling process:

Equations of Motion: - The mechanical dynamics of the motor can be described by Newton's second law $J * \frac{dW}{dt} = T_e - T_l$

Electromagnetic Torque: - The electromagnetic torque for an IPMSM can be expressed as: $T_e = \frac{3}{2} * \frac{P}{2} * (\lambda_{pm} i_q + (L_q i_d i_q)$

Voltage Equations:- The voltage equations in the d-q reference frame can be expressed as:$U_d = R_s i_d + L_d \frac{di_d}{dt} - W_e \lambda_{pm}$ & $U_q = R_s i_q + L_q \frac{di_q}{dt} + W_e L_d i_d$

State-Space Representation: To investigate the system, it is frequently useful to convert the equations into a state-space representation. Defining state variables $x = [i_d, i_q, We]^T$. The state equations can be written as follow $\frac{dx}{dt} = Ax + Bu$ and $y = Cx + Du$

Simulation and Control: - The mathematical model can be implemented in simulation tools like MATLAB/Simulink to investigate the system's behaviour under different operating conditions. Control strategies, such as vector control or direct torque control, can be planned based on the model. This basic model offers a framework to understand the behaviour of IPMSMs. More complex models may include effects like saturation, temperature dependence, and nonlinearities, depending on the mandatory accuracy and application.

Three Phase Mathematical Modelling of IPMSM

IPMSM has an inherent magnetic saliency property that increases torque production because of the PM inside the rotor core. The total of the voltage drop across the stator winding is the supply voltage of the winding. The back-EMF is the induced voltage.

$$L_q = \frac{\mu_0 N^2 A}{2(g)} \qquad 2.3$$

$$\lambda_{pm} = L_d i_f$$

A mathematical model of the IPMSM is used in order to simulate the behaviour of the machine in MATLAB/Simulink. The d-axis of the model is aligned with the rotor flux-linkage in the dq rotor reference frame. In stator coordinates, the IPMSM's voltage stator-phase equations [1]. Thus, the phase variable's frame the three-phase model is framed by the voltage equation as follows:

.

$$U_a = R_s i_a = \frac{\partial \lambda_a}{\partial t} \qquad 2.4 \text{ A}$$

$$U_b = R_s i_b = \frac{\partial \lambda_b}{\partial t} \quad \text{B}$$

$$U_c = R_s i_c = \frac{\partial \lambda_c}{\partial t} \quad \text{C}$$

$U_a,\ U_b,\ U_c$ are the stator phase voltage Rs is the stator resistance and $\lambda_a,\ \lambda_b,\ \lambda_c$ they are the phase flux linkages. The flux equation of each phases is be come

$$\lambda_a = L_{aa} i_a + M_{ab} i_b + M_{ac} i_c + T_e \quad \text{2.5 A}$$

$$\lambda_b = M_{ba} i_a + L_{bb} i_b + M_{bc} i_c + \lambda_{pmb} \quad \text{B}$$

$$\lambda_c = M_{ca} i_a + M_{cb} i_b + L_{cc} i_c + \lambda_{pmc} \quad \text{C}$$

The permanent magnet flux can be expressed: -

$$\lambda_{pma} = \lambda_{pm}\, cos(\theta) \quad \text{2.6 A}$$

$$\lambda_{pmb} = \lambda_{pm} cos(\theta - 120^0) \quad \text{B}$$

$$\lambda_{pmc} = \lambda_{pm}\, cos(\theta + 120^0) \quad \text{C}$$

When leakage inductance is negligible, the phase inductance in an IPMSM (Interior Permanent Magnet Synchronous Motor) can indeed be modeled as a function of the rotor's electrical angle θ\theta. This is due to the rotor's anisotropic structure, where the magnetic reluctance varies with its position. The phase inductance can generally be expressed as:

$$L_{aa}(\theta) = L_l + L_m - L_{hm} cos(\theta) \quad \text{2.7 A}$$

$$L_{bb}(\theta) = L_l + L_m - L_{hm} cos(\theta - 120^0) \quad \text{B}$$

$$L_{cc}(\theta) = L_l + L_m - L_{hm} cos(\theta + 120^0) \quad \text{C}$$

The mutual inductance between different phase can be expressed: -

$$L_{ab}(\theta) = -\frac{1}{2} L_m - L_{hm} cos2(\theta - 120^0) \quad \text{2.8 A}$$

$$L_{ac}(\theta) = -\tfrac{1}{2} L_m - L_{hm} cos2(\theta + 120^0) \quad \text{B}$$

$$L_{bc}(\theta) = -\frac{1}{2} L_m - L_{hm} cos2(\theta) \quad \text{C}$$

The Back-EMF of IPMSM can be presented by the following Fourier series L_l Stator self-inductance, there value is the same. L_m & L_{hm} It is given as average magnetization and half magnetization respectively. $-\frac{1}{2}$ Appears all the phases are phase shifted by 120^0 because the value of $cos \pm 120^0$ is $-\frac{1}{2}$.

$$L_m = \frac{1}{2}(L_q + L_d) \quad \text{2.9 A}$$

$$L_{hm} = \frac{1}{2}(L_q - L_d) \quad \text{B}$$

R_s & λ_{pm} Also change when the temperate change

$$\lambda = \lambda_{25^0}(1 - \alpha_\lambda \Delta T) \quad \text{2.10 A}$$

$$R = R_{25^0}(1 + \alpha_\lambda \Delta T) \quad \text{B}$$

2.5.1 Transformation

By altering the reference frame of stator current vectors, mathematical methods known as Clarke and Park transforms make motor control easier in Field-Oriented Control (FOC). Here's a brief summary. The three-phase stator currents (a, b, and c) are transformed into a two-axis stationary reference frame (α, β) using the Clarke Transform. In order to simplify three-phase signals, this step is crucial. In order to align the rotor flux with the revolving reference frame (d, q), the Park Transform further spins the stationary (α, β) frame. The component that produces flux in this frame is usually handled by the d-axis, while the component that produces torque is handled by the q-axis. Similar to controlling a DC motor, FOC provides quick, accurate, and decoupled torque and flux control by independently regulating the d- and q-axis currents. This is especially effective for high-performance uses like Here's a brief summary:

The mathematical model and control scheme of IPMSM utilize there is two main transformation that's are Clark Transformation and Park Transformation

The changes of Three-axis coordinate into Two-axis stationary and Orthogonal coordinate system as $\alpha\beta$. This changing axis Stator reference coordinates system to be two-axis orthogonal system referred to $dq - axis$

2.5.2 Clarke Transformation

Clarke transform uses three-phase currents i_a, i_b and i_c to calculate currents in the two-phase orthogonal stator axis$i\alpha \; and \; i\beta$. These two currents in the fixed coordinate stator phase are transformed to the $i_s d \; and \; i_s q$ currents components in the dq frame with the Park transform. These currents i_{sd}, i_{sq} and the instantaneous flux angle,

calculated by the motor flux model, are used to calculate the electric torque of an IPMSM the currents can be considered as components of stator current.

$$\boldsymbol{i_s} = \begin{bmatrix} i_a \\ i_b \\ i_c \end{bmatrix} \qquad 2.11$$

The mathematical transformation called Clarke transform modifies a three-phase system to a two-phase orthogonal system:

$$i_\alpha = \frac{2}{3} i_a - \frac{1}{3}(i_b - i_c) \qquad 2.12 \text{ A}$$

$$i_\beta = \frac{2}{\sqrt{3}}(i_b - i_c) \qquad \text{B}$$

$$i_o = \frac{2}{3}(i_a + i_b + i_c) \qquad \text{C}$$

Where: - i_α and i_β the homopolar component of the system and components in an orthogonal reference frame. The homo polar component is either nonexistent or of lesser significance in many applications. In this manner, the original three-phase input signal is represented by the space vector u = $ua + jub$ when there is no homopolar component. Examine a specific instance where i_a is superposed i_a and $i_a + i_b + i_c$ equals zero. In this scenario, i_a, i_b, i_c can be transformed to i_a, i_b with the use of the following mathematical transformation.

$$i_\alpha = i_a \qquad 2.13 \text{ A}$$

$$i_\beta = \frac{1}{\sqrt{3}} i_a + \frac{2}{\sqrt{3}} i_b \qquad \text{B}$$

$$i_a + i_b + i_c = 0 \qquad \text{C}$$

Need to represent into two axis form α & β.

Clark Transformation also considered as a process which take three phase coils describe 120^0 into two coil form and orthogonal each other

2.5.3 Park Transformation

The two phases' frame representations, $a\ and\ b$, are transformed using the mathematical park transform. The resulting representation is then supplied into a vector rotation block, which rotates it over an angle θ in order to follow the dq frame connected to the rotor flow. The following formulas are used to perform the rotation over an angle dq. This conversion used to control purpose the current vector to modify represent $dq - axis$ that will be synchronous with rotation of the rotor.

$$\boldsymbol{i_s} i_d = I_\alpha cos\theta + i_\beta sin\theta \quad \text{2.14 A}$$

$$i_q = I_\alpha sin\theta + i_\beta cos\theta \quad \text{B}$$

Sinusoidal current obtains at two axes be have at the steady state DC value. According to rotor flux angle θ_r that is measured with respect to any arbitrary component of current do not change with the change in time as $dq - frame$ is rotating along the reference frame of rotor and the limitation of control at high speed do not exist.

$$\begin{bmatrix} U_q \\ U_d \end{bmatrix} = \frac{2}{3}\begin{bmatrix} -sin\theta_r & -sin(\theta_r - 120^0) & -sin(\theta_r + 120^0) \\ cos\theta_r & cos(\theta_r - 120^0 & cos(\theta_r + 120^0) \end{bmatrix}\begin{bmatrix} u_a \\ u_b \\ u_c \end{bmatrix} \quad \text{2.15}$$

$$\begin{bmatrix} u_a \\ u_b \\ u_c \end{bmatrix} = \begin{bmatrix} -sin(\theta_r) & cos(\theta_r) \\ -sin(\theta_r - 120^0) & cos(\theta_r - 120^0) \\ -sin(\theta_r + 120^0) & cos(\theta_r + 120^0) \end{bmatrix}\begin{bmatrix} U_q \\ U_d \end{bmatrix} \quad \text{2.16}$$

U_d , U_q are the stator voltage vector's d and q components. The angle between the rotor's revolving d-axis and the stator's stationary a-axis is denoted by θ. Some principle with voltage equation we do for current equation. The rotor flux simply controlled by i_d and Torque be controlled by the manipulator of i_q.

The i_d , i_q are the stator current vector's d and q components. θ is the angle formed by the rotor's revolving d-axis and the stator's stationary a-axis.

$$\begin{bmatrix} i_q \\ i_d \end{bmatrix} = \frac{2}{3}\begin{bmatrix} -sin\theta_r & -sin(\theta_r - 120^0) & -sin(\theta_r + 120^0) \\ cos\theta_r & cos(\theta_r - 120^0 & cos(\theta_r + 120^0) \end{bmatrix}\begin{bmatrix} i_a \\ i_b \\ i_c \end{bmatrix} \quad \text{2.17}$$

The vector picture of the transformation is obtainable.

$$\begin{bmatrix} i_a \\ i_b \\ i_c \end{bmatrix} = \begin{bmatrix} -sin(\theta) & cos(\theta) \\ -sin(\theta - 120^0) & cos(\theta - 120^0) \\ -sin(\theta + 120^0) & cos(\theta + 120^0) \end{bmatrix}\begin{bmatrix} i_q \\ i_d \end{bmatrix} \quad \text{2.18}$$

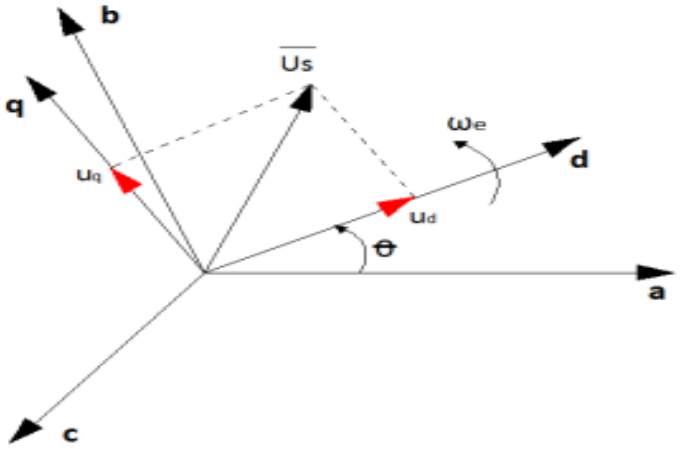

Figure 2-4: Vector representation of the abc to dq frame transformation

Where $\omega_r = \frac{d\theta}{dt}$ is the synchronous electrical speed?

On the Direct and Quadrant coordinate Dynamic modelling of the IPMSM. The space vector can be used effectively to model IPMSM.

The zero-sequence component between the stator winding and the neutral point, which is zero, is not included in the space vector. Three phase machine deference of 120 degree between phases that can be represent by α. The value of alpha is become $\alpha = e^{\frac{j2\pi}{3}}$ The stator flux linkage $\lambda_d and\ \lambda_q$ vary from $dq - axis$ and also depends on the corresponding current component

$$\lambda_d = L_d i_d + \lambda_{pm} \qquad 2.19\ A$$

$$\lambda_q = L_q i_q \qquad B$$

$d - axis$ … Is aligned with permanent magnet is adds the current produced $d - axis$ direction to need weakening in order to go high speed

Total stator flux can be calculated.

$$\lambda_s = \sqrt{\lambda_d^2 + \lambda_q^2} \qquad 2.20\ A$$

$$\lambda_s = \sqrt{\left(L_d i_d + \lambda_{pm}\right)^2 + \left(L_q i_q\right)^2} \qquad B$$

We can Apply Both Clark and Park transformations that are commonly used in Vector control of AC motors, Synchronous machine control, Harmonic analysis, Power quality assessment. These transformations help simplify the mathematical modelling of systems, making it easier to design control algorithms and perform system analysis.

2.6 The dynamic model of IPMSM

Synchronous motors operate at a constant speed irrespective of the load, making them highly efficient and ideal for high-precision applications [25]. This constant speed is achieved through the interaction of a constant rotor magnetic field and a rotating stator magnetic field, generated by a three-phase AC supply. The rotor produces a constant magnetic field, while the stator creates a revolving magnetic field that rotates at synchronous speed [26]. To model this behaviour, a $dq - frame$ is used, where the rotor flux aligns with the d-axis and the q-axis is 90^0 electrical degrees ahead, with no rotor flux along the $q - axis$. Clarke and Park Transformations are applied to convert the three-phase frame into dq, allowing for the formulation of the stator equations in relation to the rotor.

Voltage equations are given by [27].

$$u_{ds} = R_s i_d + \frac{\partial}{\partial t}\lambda_d - \omega_e \lambda_q$$
$$u_{qs} = R_s i_q + \frac{\partial}{\partial t}\lambda_q - \omega_e \lambda_d \qquad 2.21$$

Substitute the Upper equation and it gives

$$u_d = R_s i_d + \frac{\partial}{\partial t}\left(L_d i_d + \lambda_{pm}\right) - \omega L_q i_q$$
$$u_q = R_s i_q + \frac{\partial}{\partial t}(L_q i_q) - \omega_r L_d i_d + \omega_r \lambda_{pm} \qquad 2.22$$

The matrix form of the upper equation becomes

$$\begin{bmatrix} u_d \\ u_q \end{bmatrix} = \begin{bmatrix} R_s + \frac{\partial}{\partial t}\lambda_d & -\omega_r L_q \\ \omega_r L_d & R_s + \frac{\partial}{\partial t}\lambda_q \end{bmatrix} \begin{bmatrix} i_d \\ i_q \end{bmatrix} + \omega \begin{bmatrix} 0 \\ \lambda_{pm} \end{bmatrix} \qquad 2.23$$

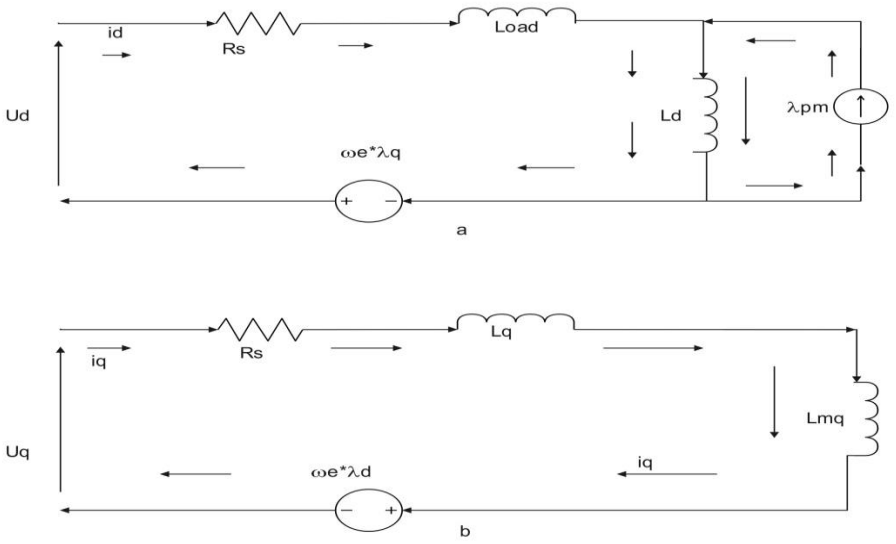

Figure 2-5: - Equivalent circuit of dq voltage equation frame of an IPMSM

The $dq - axis$ stator current

$$\frac{\partial i_d}{\partial t} = \frac{1}{L_d}\left[-R_s i_d + \frac{P}{2}\omega_r L_q i_q + u_d\right]$$
$$\frac{\partial i_q}{\partial t} = \frac{1}{L_q}\left[-R_s i_q + \frac{P}{2}\omega_r (L_d i_d + \lambda_{pm}) + u_q\right] \quad 2.24$$

We can re-write the upper equation in the integral equation form

$$i_d = \int \frac{1}{L_d}\left[-R_s i_d + \frac{P}{2}\omega_r L_q i_q + u_d\right]$$
$$i_q = \int \frac{1}{L_q}\left[-R_s i_q + \frac{P}{2}\omega_r (L_d i_d + \lambda_{pm}) + u_q\right] \quad 2.25$$

From this equation we can develop our modelling block circuit diagram of the MATLAB simulation

2.7 The mechanical Modelling of the IPMSM

The general mechanical equation for the IPMSM is as follow is used to develop the Torque equation and electrical speed equation.

$$\frac{d\omega_e}{dt} = -\frac{B}{J}\omega_r + \frac{1}{J}(T_e - T_l) \quad 2.26$$
$$\omega_e = \int \frac{(T_e - B\omega_r - T_l)}{J} \quad [29]$$

This gives as $\frac{d\theta}{dt} = \omega_e$ and also for rotor speed we use $\omega_e = \frac{P}{2} * \omega_r$

And the torque equation developed from the mechanical speed equation

$$T_e = T_l + T_d + B\omega_r + J\omega_e \qquad 2.27$$

This torque equation used to develop the sliding mode control for the use of controlling designed purpose

The general IPMSM Mathematical Model that Combining the equations and make a matrix form we can put in following forms:

$$\frac{d}{dt}\begin{bmatrix} i_d \\ i_q \\ \omega_e \\ \theta_r \end{bmatrix} = \begin{bmatrix} \frac{1}{L_d}(-R_s) & \frac{1}{L_d}(\omega L_q) & 0 & 0 \\ \frac{1}{L_q}(\omega L_d) & \frac{1}{L_q}(-R_s) & 0 & 0 \\ 0 & 0 & -\frac{B}{J} & 0 \\ 0 & 0 & 0 & 0 \end{bmatrix}\begin{bmatrix} i_d \\ i_q \\ \omega_r \\ \theta_r \end{bmatrix} + \begin{bmatrix} \frac{1}{L_d}(u_d) \\ 1/L_q(u_q - \omega_r\lambda_{pm}) \\ \frac{1}{J}(T_e - T_l) \\ \omega_r \end{bmatrix} \qquad 2.28 \text{ [1]}$$

2.8 The IPMSM Mathematical model verification simulation

To checked the behaviour of the machine at different torque level and different speed level the implemented mathematical model of IPMSM on MATLAB Simulink is needed. For the next chapter presented the overall control model is used to the Simulink model. The block diagram used to show the stricter of simulation model.

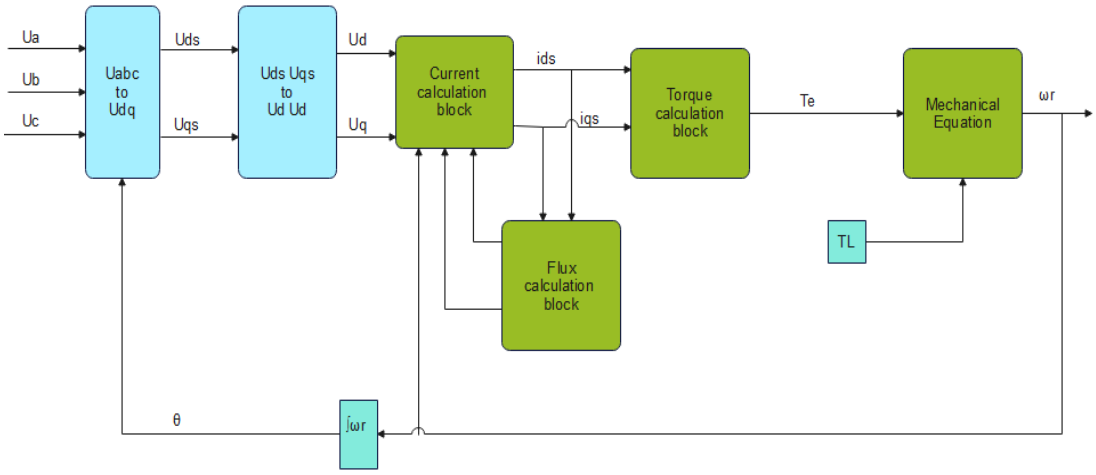

Figure 2-6: Block diagram shows the representation of Simulink model of IPMSM

For the input of the rotor speed and stator current are the modelling outputs of the IPMSM simulation model, which uses a sin function to calculate the phase voltage. The applied phase voltages that flow from sin function we call it u_a, u_b, and u_c are transformed in to the $dq - axis$ component using the abc to dq frame transformation method. Using rearrange stator voltage equation and flux equation we can expressed the stator current as follow

After drive the current equation drown the current calculation block on MATLAB Simulink. Also, from driven flux equation drown the flux calculation block on MATLAB Simulink. Having the known currents ids and iq the produced electromagnetic torque and angle θ_r can be calculated. If the mechanical equation presented then considered it, the speed rotor can be calculated.

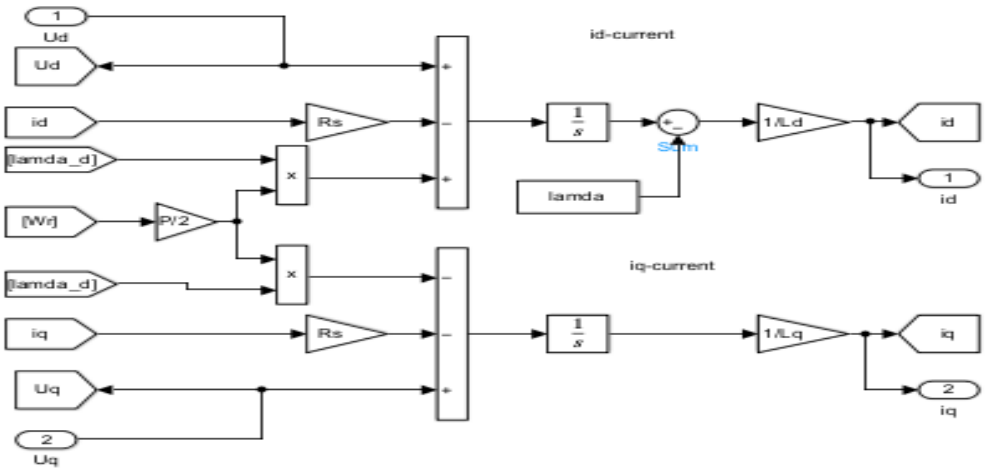

Figure 2-7: - The id and iq current equation in block diagram form.

After having the Known i_{dq} currents, the torque equation can be used to compute the generated torque. The shaft speed can be computed as follows if the mechanical equation shown in is also taken into account:

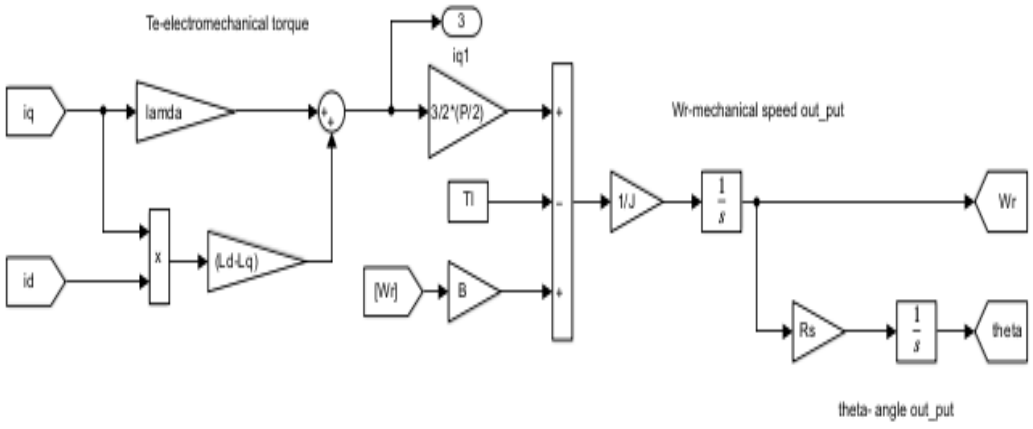

Figure 2-8: - The speed equation in block diagram form.

Table-1 Parameters of the tested IPMSM

Roll number	Parameter	Value

1	Rated Torque	400N.m
2	Rated speed (ω_e)	314rpm
3	Number of pole pairs	4
4	Rated DC voltage (u_{dc})	550volt
5	Maximum Speed (ω_{e-max})	628rpm
6	Permanent magnet flux linkage (λ_{pm})	0.1757volt/sec
7	Stator resistance per phase (R_s)	6.5e-3Ohm
8	q-axis inductance (L_q)	2.057e-3mH
9	d-axis inductance (L_d)	1.597e-3mH
10	The moment of inertia (J)	0.09(Kg.m^2)
11	Friction coefficient ($\boldsymbol{B}$)	0.002(Nm/s)

Model verification result

The model verification of the IPMSM lacked information on its working point. To evaluate the machine's behaviour, the IPMSM model was tested at different load torques and speeds, using electrical parameters from the upper Table. For simplicity. The analysis began with Clarke and Park coordinate transformations, commonly used in Field Oriented Control of three-phase AC machines. The Clarke transform converts a three-phase system in the $abc-frame$ to two components in the orthogonal stationary $\alpha\beta-frame$, while the Park transform further converts these components into the rotating dq reference frame. Using these transforms consecutively simplifies the computation by turning AC current and voltage waveforms into DC signals.

No-Load Test Summary for IPMSM The IPMSM model was initially tested under no-load conditions. It achieved a steady-state speed of 314.2 rad/s. As illustrated in the corresponding figures, the amplitude of the stator phase voltage was 550 V, while the stator current peaked at 231.5 A.

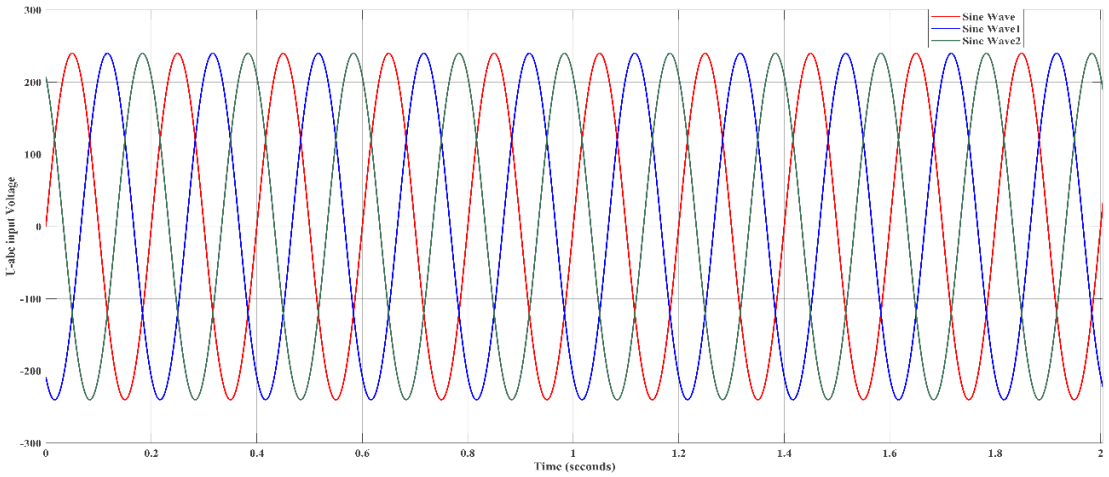

Figure 2-8: -The time domain components of a three-phase system (in abc frame)

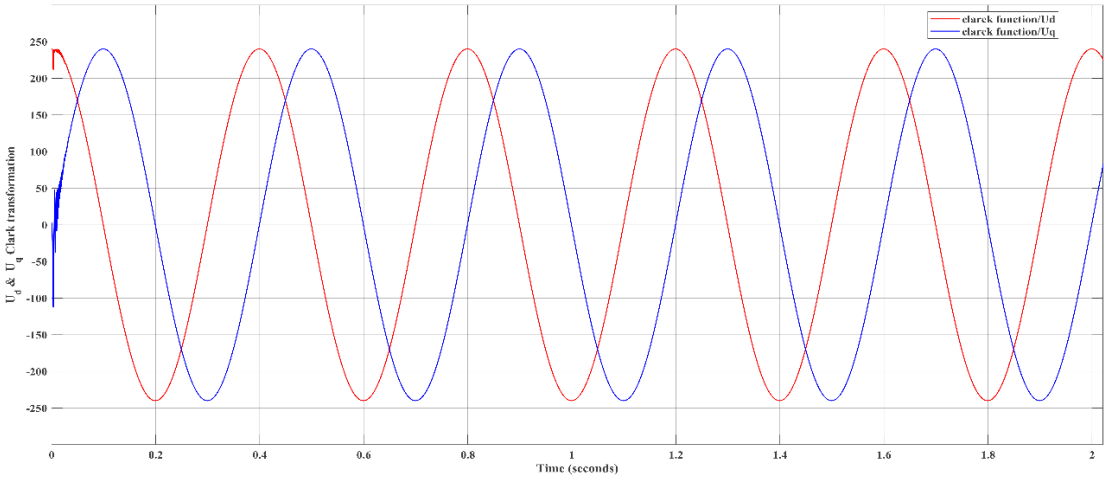

Figure 2-9: - Resulting signals for the Clarke transform(αβ) on dq frame.

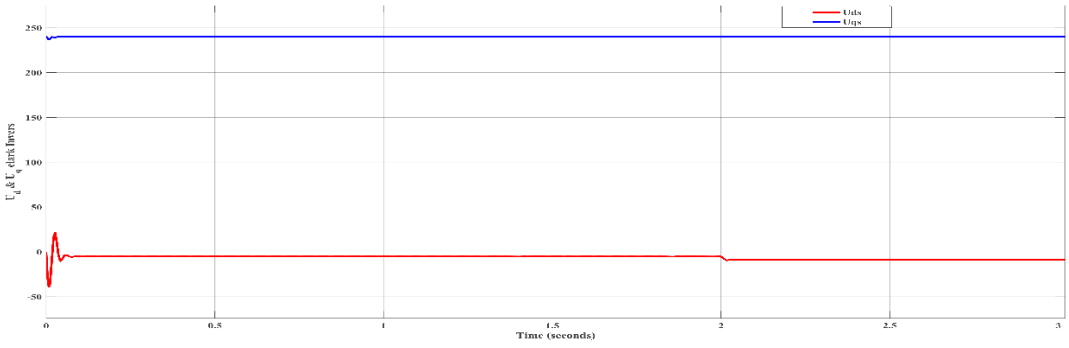

Figure 2-10: -Resulting signals for the Park transform (dq)

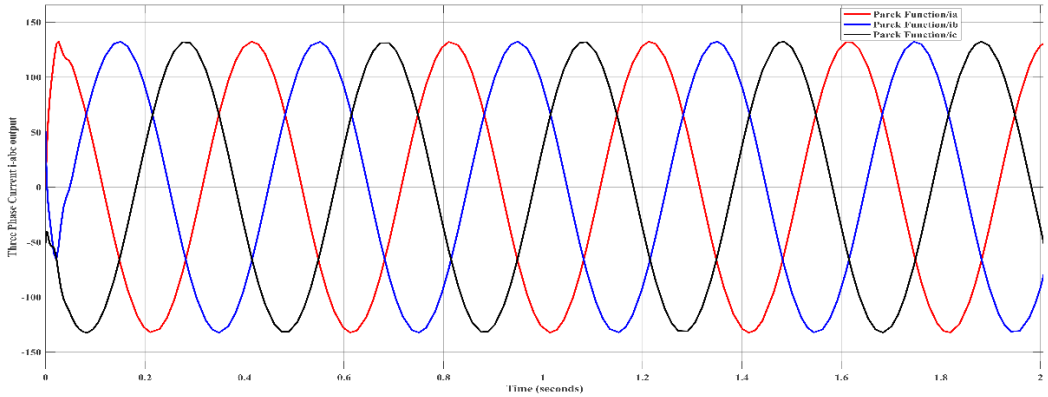

Figure 2-11: - shows three Phase current at no-load (Tl=0)

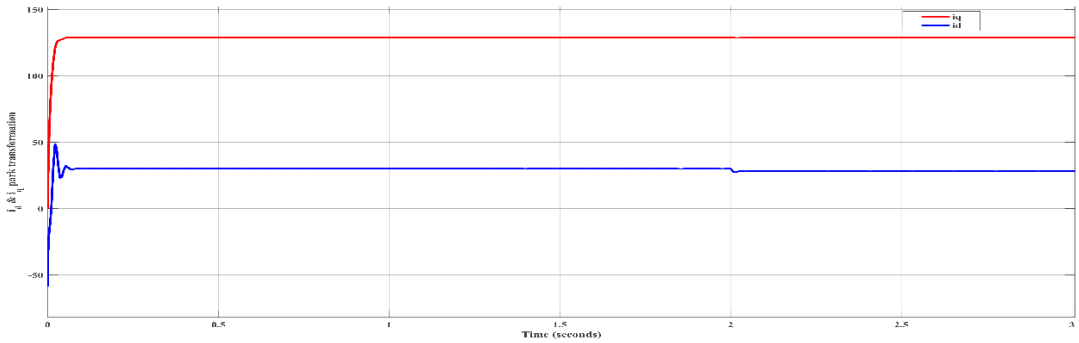

Figure 2_12: - the Clark transformation on the current that shows No-load torque and 20N-m load torque

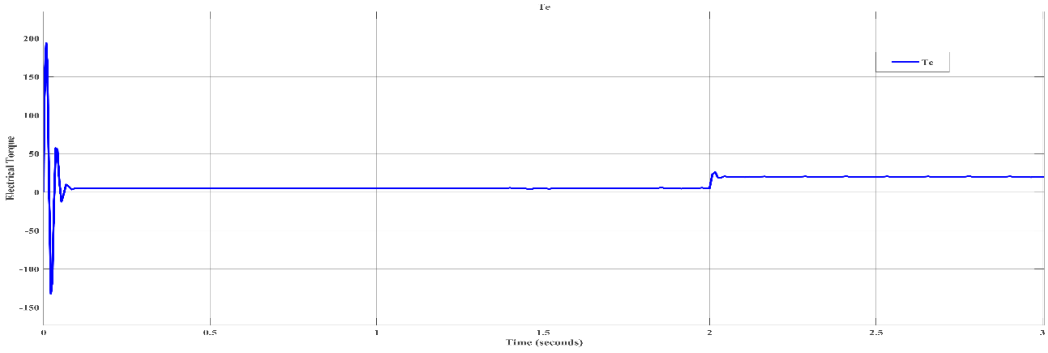

Figure 2-13: Shows Electrical torque when load torque changes from 5N-m to 20N-m

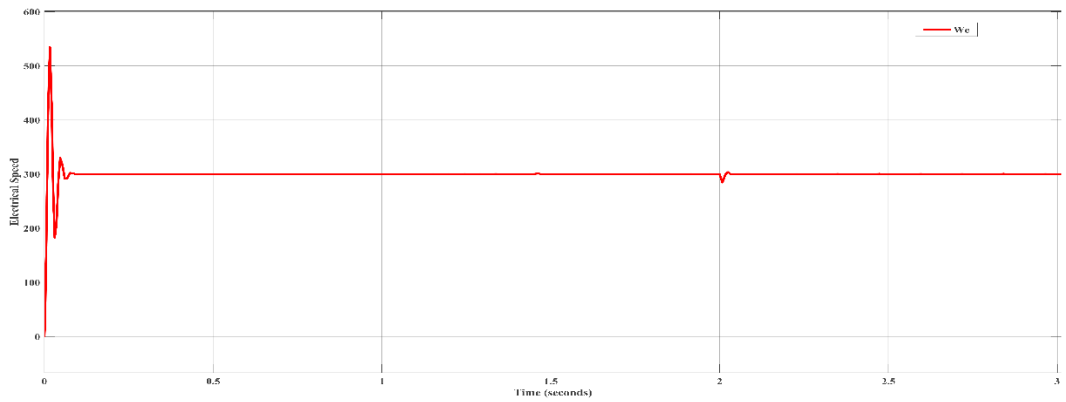

Figure 2-14: shows electromagnetic speed at no-load (Tl=0) and 20N-m load torque

At load torque is 20N-m the phase voltage becomes 123.25volt and the phase current becomes 64.8Ampere.but the speed had no change with no load torque test.

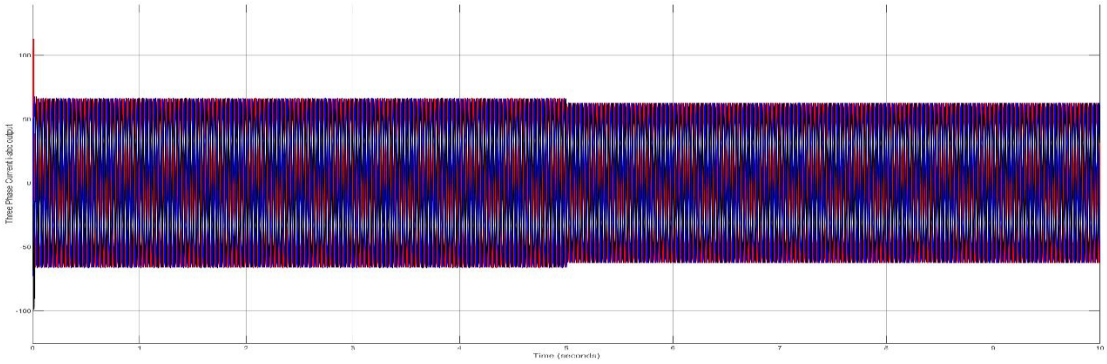

Figure 2-15: Three phase current output at no-load torque 0N-m and 20N-m load torque

Consideration of Real-World Control Implementation A three-phase inverter with a 192 V DC-link powers the IPMSM. The largest phase voltage amplitude that may be achieved with space vector modulation (SVM) is roughly 111 V. The observed phase voltage in the load test at 1200 rpm was quite close to this limit, highlighting how crucial voltage margin is in controller design. IPMSM Test and Modeling Conclusion Simulation tests show that the IPMSM can handle a load of up to 15 Nm at 1200 rpm before reaching the maximum voltage limit of the inverter. When under load, the motor's nominal working range is anticipated to be between 300 and 1200 rpm. Depending on present limitations, larger torque might be possible at lower speeds. In order to assess motor performance at different speeds and loads, this chapter also presented the main features of the IPMSM, developed its mathematical model in the dq reference frame, and implemented it in MATLAB/Simulink.

CHAPTER – Three

3 Interior Permanent Magnet Synchronous Motor Control

3.1 Interior Permanent Magnet Synchronous Motor controllers

An examination of the IPMSM's torque production mathematical equation. The Interior Permanent Magnet Synchronous Motor (IPMSM) features permanent magnets embedded inside the rotor, providing improved efficiency, compactness, and performance, especially for applications like electric vehicles (EVs) and industrial drives [27]. It includes Current Control used to Regulates motor performance by controlling the stator current to achieve desired torque and speed. Speed and Position Control is Uses sensors like encoders or resolvers to monitor rotor position for precise control. Maximum Torque per Ampere (MTPA) Control is to Maximizes torque output for a given current, increasing efficiency by reducing energy consumption. Wide Range Speed Control is to allows the motor to maintain efficient operation across a broad speed range, ensuring stability and performance from low to high speeds. In IPMSM motor controller design, key control strategies include. Field-Oriented Control (FOC) Offers efficient and precise torque and flux control [28].

Direct Torque Control (DTC) Provides fast dynamic response but is more complex.

Vector Control is Controls motor flux and torque independently for optimal performance.

Under controller designing includes current control tuning and speed control designing. For current control designing PI Control Combines proportional and integral actions to minimize steady-state error and ensure system stability but for this thesis we use PI current tuning under speed control designing. we are applying this two controllers Sliding Mode Control (SMC) which is uses for robust technique that forces the system's state to a predefined sliding surface [29], ensuring high robustness against disturbances and uncertainties. And the second one is Integral Sliding Mode Control (ISMC) used to Enhances SMC by adding an integral term to address steady-state errors and external disturbances while preserving robustness.

3.2 Maximum torque per ampere (MTPA) Control of IPMSM

The fundamental idea behind any electrical motor control is to maintain the intended speed regardless of variations in the applied load torque. Controlling the torque that

the motor produces is necessary to achieve the desired speed. investigating the IPMSM's torque production mathematical equation.

$$T_e = \frac{3}{2}P\left[(\lambda_{pm})i_q + (L_d - L_q)(i_q i_d)\right] \quad 3.29$$

Where: - T_e- Electrical Torque P- Pair of Pole

λ_{pm} -Permanent Magnet Flux L_d -d-Inductance

L_q – q-Inductance i_q – q-Current i_d -d-Current

The torque in an IPMSM is controlled by the current components i_q and i_d, assuming constant inductances L_d and L_q. The IPMSM is a typical AC motor, featuring dispersed windings in the stator slots that, when powered by a three-phase, balanced voltage system, produce a revolving magnetic field. Therefore, permanent magnet motors can be driven using the same main motor control techniques as are used to drive induction motors. The four main methods for motor control are:

A. **Variable Frequency Drive (VFD)**

U/f control adjusts the motor power supply voltage and frequency to maintain constant magnetic flux, ensuring efficient speed regulation without decreasing power factor. However, its low-speed performance is limited.

B. **Slip Frequency Control**

This method controls torque and current by managing the slip frequency, the difference between AC power frequency and motor speed. It requires speed detection and a closed-loop system for improved acceleration, deceleration, and overcurrent protection compared to U/f control.

C. **Vector Control in Closed Loop or Field Oriented Control (FOC)**

FOC separates torque and flux control for exact, efficient, and dynamic motor control, ideal for high performance applications. It uses real time feedback for motor speed and torque control, similar to DC motors but without commutators, and is commonly used in electric vehicles and industrial systems.

D. **Direct Torque Control (DTC) in Closed Loop**

DTC directly controls torque, overcoming vector control limitations. It adjusts stator flux linkage without needing speed information and remains robust against motor parameter changes, except for stator resistance, making it highly efficient for high-performance applications.

Maximam torque per ampire (MTPA) control scheme

PMSMs are categorized into two types based on rotor magnet placement: Surface Mounted Permanent Magnet Synchronous Motor (SPMSM) and Interior Permanent Magnet Synchronous Motor (IPMSM).

Interior mounted permanent magnet Synchronous Motor (IPMSM): - The $d-axis$ and $q-axis$ inductance values differ, and the rotor is salient. IPMSMs can generate both reluctance and magnet-based torque. Proper use of reluctance torque improves efficiency and motor performance.

Surface mounted permanent magnet Synchronous Motor (SPMSM): - The rotor is non-salient, with no $d-axis$ and $q-axis$ inductance difference. They only produce torque from permanent magnets, controlled using Field-Oriented Control (FOC) with the $Id = 0$ strategy. Reluctance torque is not present in SPMSMs.

The Maximum Torque Per Ampere (MTPA) strategy optimizes torque by controlling the reluctance torque. The MTPA Control Reference block computes the necessary $d-axis$ and $q-axis$ current for efficient torque generation and supports both maximum torque and field-weakening operations.

The Operation Principle of Maximum Torque Per Ampere (MTPA)

MTPA and DTC are the most often used control techniques for IPMSM. By choosing the proper inverter state, DTC directly regulates stator flux and torque. By regulating stator current, MTPA seeks to maximize torque while consuming the least amount of current. These techniques may result in better performance. The Maximum Torque Per Ampere (MTPA) control strategy goals are to maximize the torque produced by a Permanent Magnet Synchronous Motor while minimizing the current required. The operation principle of MTPA focuses on the optimal control of the stator current to achieve the maximum possible torque for a given current magnitude. It means to optimizes the $d-axis$ and $q-axis$ stator currents to reach the maximum torque for a given current. MTPA adjusts the $d-axis$ and $q-axis$ currents to maximize torque while minimizing energy input to optimize current using the torque formula on equation (2.1). Current Angle is an optimal angle between the current vector and the $q-axis$ to maximizes torque and minimizes losses. MTPA optimally manages reluctance torque arising from inductance differences in the $dq-axes$. It works with speed and torque control to ensure efficient motor operation across various loads.

MTPA improves torque while reducing energy consumption, improving IPMSM efficiency [2].

Maximum torque per ampere scheme as can be seen in equation (2.2), torque in salient pole Permanent Magnate machines has two different components. The first component is the result of the interaction between the $q-axis$ current and the permanent magnet flux linkage while the second one is the reluctance torque which is due to the difference in the inductance between the $d\ and\ q\ axes$ [1].

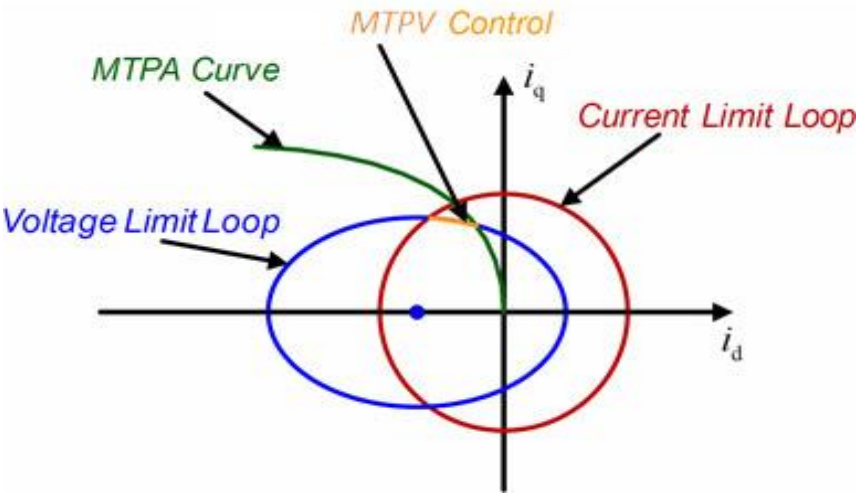

Figure 3-1: - MTPA curve of Interior PMSM.

For every load torque, there exists an optimal current angle that maximizes the torque for a given current magnitude and minimizes the motor's copper loss. This optimal current angle is known as the MTPA (Maximum Torque per Ampere) angle (θ), which is defined as the angle between the current vector and the $q-axis$. The MTPA angle can be derived by considering the direct and quadrature axis components of the armature current, which can be expressed as follows: -

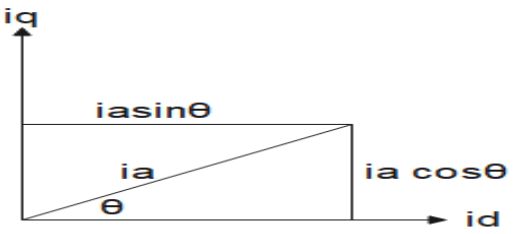

To calculate the value of i_d & i_q in polar form by substitution $i_d\ and\ i_q$ by polar form equation forms by used the upper picture end this equation $|I_a| = \sqrt{i_d^2 + \mathrm{i}_\mathrm{q}^2}$

$$T_e = \frac{3P}{2}\left[(\lambda_{pm})i_q + (L_d - L_q)(i_q i_d)\right]$$
$$i_d = I_a sin\theta$$
$$i_q = I_a cos\theta \qquad 3.30$$

$I_a = I_s = i_{max}$ … … … … magnitude of armature current per phase

Vector frame aligned with the induced voltage hence, the torque equation becomes equation (2.3): -Substituting the value of $i_q, i_d,$ & i_s on the Torque equation

$$T_e = \frac{3P}{2}\left[(\lambda_{pm})I_a cos\theta\ + (L_d - L_q)(I_a cos\theta\ I_a sin\theta)\right]$$
$$T_e = \frac{3P}{2}\left[(\lambda_{pm})I_a cos\theta\right.$$
$$\left. + (L_q - L_d)I_a cos\theta^2\ (I_a sin\theta)^2)(I_a cos\theta\ I_a sin\theta)\right] \qquad 3.31$$
$$T_e = \frac{3P}{2}\left[(\lambda_{pm})I_a cos\theta\ + (L_q - L_d)I_a^2 sin2\theta\right)$$

It has two torque results those are due to permanent magnet synchronies torque and reluctance torque due to the saliency

$$T_{pm} = \frac{3P}{2}\left[(\lambda_{pm})I_a cos\theta\right.$$
$$T_{REL} = \frac{3P}{2}(L_d - L_q)I_a^2 sin2\theta) \qquad 3.4$$

I_a …$produce\ exitation\ torque(Magnetic\ Torque)$

I_a^2 …$produce\ relactance\ torque$

Now we can drive the value of θ from the torque equation. T_{max} Vector produce the maximum torque intersect point of the maximum torque per ampere trajectory and the current limit circle and the reference $dq-$ axis stator current i_d and i_q coordinate can be dreven by taking the derivative of torque with respect to θ and equating with zero

$$\frac{\partial T_e}{\partial \theta} = 0 \qquad 3.32$$

substituting the equation leads to the following equation:

$$\frac{dT_e}{d\theta} = \frac{\frac{3P}{2}\left[(\lambda_{pm})I_a cos\theta\ + ((Ld - Lq))I_a^2 sin2\theta)\right]}{d\theta} = 0 \qquad 3.33\ A$$
$$\frac{dT_e}{d\theta} = \frac{3P}{2}\left[(-\lambda_{pm})I_a sin\theta\ + ((Ld - Lq))I_a^2 cos2\theta)\right] \qquad B$$
$$\frac{dT_e}{d\theta} = \frac{3P}{2}\left[\ (-\lambda_{pm})I_a sin\theta\ + ((Ld - Lq))I_a^2\right. \qquad C$$
$$\left. - 2((Ld - Lq))I_a^2\ sin^2\theta)\right]$$

Which leads to: -

$$\frac{dT_e}{d\theta} = \frac{3P}{2}\left[2((Ld-Lq))I_a^2\ sin^2\theta) + \left(\lambda_{pm}\right)I_a sin\theta - \left((Ld-Lq)\right)I_a^2\right] \quad 3.34$$

Using quadratic equation formula $\frac{-b\pm\sqrt{b^2-4ac}}{2a}$ we can drive the sin function

$$sin\theta = \frac{I_a\left[-\lambda_{pm} \pm \sqrt{-\lambda_{pm}{}^2 - 4\left(2((Ld-Lq))\right)I_a * ((Ld-Lq))I_a]}\right]}{2(2((Ld-Lq))I_a} \quad 3.35$$

$$sin\theta\ = -\frac{\lambda_{pm}}{4\left(L_q - L_d\right)} + \sqrt{\frac{\lambda_{pm}}{16\left((Ld-Lq)\right) * I_a^2} - \frac{I_a^2}{2}}$$

$$\theta = sin^{-1}\left[\frac{-\lambda_{pm} + \sqrt{\lambda_{pm}{}^2 + 8(((Ld-Lq))^2)I_a^2}}{4((Ld-Lq)) * I_a}\right] \quad 3.9$$

After we get the value, Substituting the value of θ into $|I_a|$ and solving for the d_axis current for MTPA point is obtained

$$i_{d-mtpa} = I_a\left[\frac{-\lambda_{pm} + \sqrt{\lambda_{pm}{}^2 + 8(((Ld-Lq))^2)I_a^2}}{4((Ld-Lq)) * I_a}\right] \quad 3.36$$

Substituting the relationship of currents $I_a^2 = i_d^{*2} + i_q^{*2}$ in to the formula i_{d-MTPA} yields and rearrange the i_{d-mtpa}current stand from the abave equation

$$i_{d-mtpa} = \left[\frac{-\lambda_{pm}}{2((Ld-Lq))} + \sqrt{\frac{\lambda_{pm}^2}{4(Ld-Lq)^2)} + i_q^2}\right] \quad 3.37$$

When substitute the upper i_{d-mtpa} current equation in to electromagnetic torque equation on that formulated by $I_a = \sqrt{i_d^{*2} + i_q^{*2}}$ and it gives $i_q = \sqrt{I_a^2 - i_d^{*2}}$ and substitute I_{max} and we can drive the gate following equation by Substitute the value of i_d^{*2}

$$i_{q-mtpa} = \sqrt{I_a^2 - \left[\frac{\lambda_{pm}}{4((Ld-Lq))} + \sqrt{\frac{\lambda_{pm}}{16((Ld-Lq)^2)} - \frac{I_a^2}{2}}\ \right]^2} \quad 3.38$$

Therefore, IPMSM can achieve the maximum torque per ampere by computing $q-axis\ and\ d-axis$ Reference current from torque equation (2.29) then the electromagnetic torque equation be coming

$$T_e = \frac{3}{4}P * i_q\left(\sqrt{\lambda_{pm}^2 + 4 * \left(L_d - L_q\right)^2\left(i_q^2\right)} + \lambda_{pm}\right)$$

$$I_{a-ref} = \frac{2}{3}\left(\frac{T_{ref}}{P * \lambda_{pm}}\right) \qquad 3.39$$

[3]

$$I_{a-ref} = \frac{2}{3}\left(\frac{\frac{3P}{4}\left[\left(-\lambda_{pm}\right)I_a sin\theta\ + \left((Ld - Lq)\right)I_a^2 - 2((Ld - Lq))I_a^2\ sin^2\theta\right]}{P * \lambda_{pm}}\right)$$

$$I_{a-ref} = \frac{\left[\left(-\lambda_{pm}\right)I_a sin\theta\ + \left((Ld - Lq)\right)I_a^2 - 2((Ld - Lq))I_a^2\ sin^2\theta\right]}{2 * \lambda_{pm}}$$

There for from this perspective analysis our MTPA results

$$I_a = min\left(I_{a-ref}, I_a\right) \qquad 3.40$$

$$i_d^* = i_{d-MTPA} = i_d^* = I_a\left[\frac{\lambda_{pm}}{4(Ld-Lq)} + \sqrt{\frac{\lambda_{pm}}{16(L_d-q)^2} - \frac{I_a^2}{2}}\ \right]$$

$$i_q^* = i_{q-MTPA} = \sqrt{I_a^2 - \left[\frac{\lambda_{pm}}{4(Ld-Lq)} + \sqrt{\frac{\lambda_{pm}}{16(L_d-q)^2} - \frac{I_a^2}{2}}\ \right]^2} \qquad 3.41$$

Also, to get the $i_{q-mtpa} - axis$ current substitute tne value of i_{d-mtpa} current in to the torque equation and can drive to get the following equation.

$$i_{q-mtpa} = (Lq - Ld)^2 * i_q^4 + \frac{2}{3} * \frac{T_e}{P} * \lambda_{pm} * i_q - \left(\frac{2}{3} * \frac{T_e}{P}\right)^2 \qquad 3.42$$

The current i_{q-mtpa} can be solved for the MTPA point by using Newton Raphson method.

$$i_{q-mtpa}(n+1) = i_{q-mtpa}(n) - \frac{function\ of\ (i_{q-mtpa} * (i_{q-mtpa}(n))}{derivative\ function\ of\ \ (i_{q-mtpa}(i_{q-mtpa}(n))}$$

derivative function of $i_{q-mtpa} = 4 * \left(L_q - L_d\right)^2 * i_q^3 + \frac{2}{3} * \frac{T_e}{P} * \lambda_{pm}$

At the start of the iteration, the initial i_{q-mtpa} is set. Since magnetic torque is active early on, the current begins at zero and then increases."

$$i_{q-mtpa}(0) = \frac{2}{3} * \frac{T_e}{P * \lambda_{pm}} \qquad 3.43$$

Substituting the value of i_{q-mtpa} in the torque equation produces the reference value i_d for MTPA operation.

$$i_{d-mtpa} = -\frac{2}{3} * \frac{T_e}{P * i_{q-mtpa} * (L_d - L_q)} - \frac{\lambda_{pm}}{(L_d - L_q)} \qquad 3.44$$

The proposed block diagram for the torque control of the Interior Permanent Magnet Synchronous Motor is shown. So the comparison of i_{d-mtpa} .In the context of MTPA control, the i_d=0 strategy sets the d-axis reference current to zero, while the q-axis reference current is generated proportionally from the reference torque using a constant, K. [3].

$$K = \frac{i_q}{T_{REL}} = \frac{2}{3} * \frac{1}{P * \lambda_{pm}} \quad \ldots..K - constant \qquad 3.45$$

It is important to note that for angle θ and current i_d is correct under the assumption that the machine parameters are constant. The efficiency in practical applications may deviate slightly from the optimum, however, precise of torque control can be achieved with the use of Newton-Raphson technique.

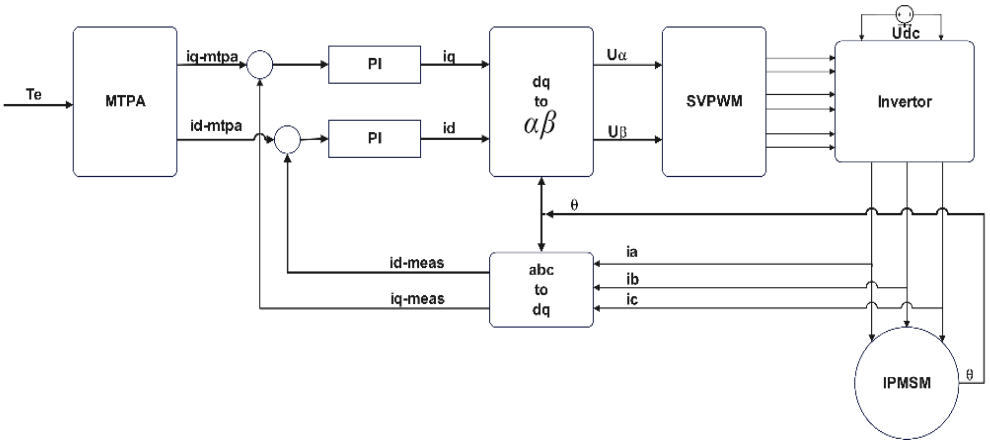

Figure 3-2: - MTPA block diagram

From equation (3.4) we driven the value of electromagnetic torque (T_e) we put the value of pair pole is equal to four (P=4) and make simplified then we draw the block diagram of MTPA.

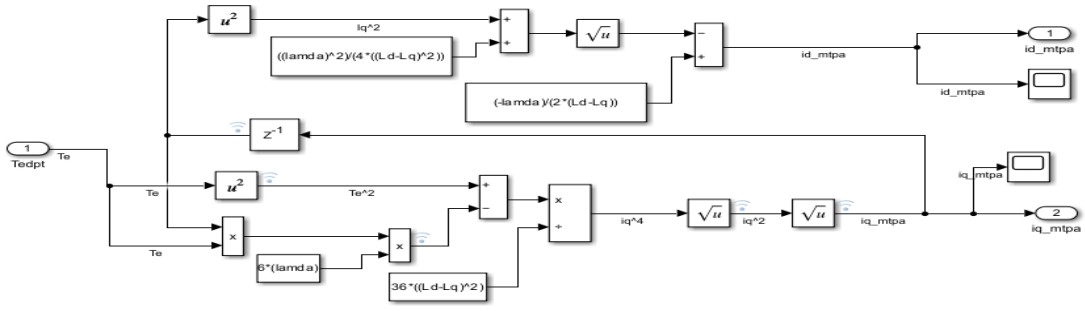

Figure 3-3: - MTPA circuit using MATLAB simulation block

The MTPA curve depends on The MTPA curve for the IPMSM is produced using important motor parameters, such as dq-axis inductances and permanent magnet flux linkage. A MATLAB program is used to derive this curve using the parameter values given in the preceding table. The maximum current (I_{max}) is set, and L_d, L_q, and λ_{pm} are treated as constants, neglecting their variations due to current or saturation, which could affect MTPA control performance in real applications [1]- [6].

Varying L_d affects the MTPA curve slope. A decrease in L_d declines the slope, increasing the $d-axis$ current (i_d) and decreasing the $q-axis$ current (i_q) for the same torque. Equally, an increase in L_d raises the slope, reducing i_d current and increasing i_q current. The MTPA curve is more sensitive to changes in L_d [1].

For inductance L_q differences, decrease in L_q increases the slope of the MTPA curve, leading to an increase in current i_q and a decrease in current i_d for the same torque. An increase in L_q declines the slope, increasing i_d and decreasing i_q [6]. The MTPA curve is more sensitive to changes in L_q. By analyzing the MTPA curve, the relationships between the torque and currents (i_{d-mtpa} and i_{q-mtpa}) can be determined for field-oriented control [28].

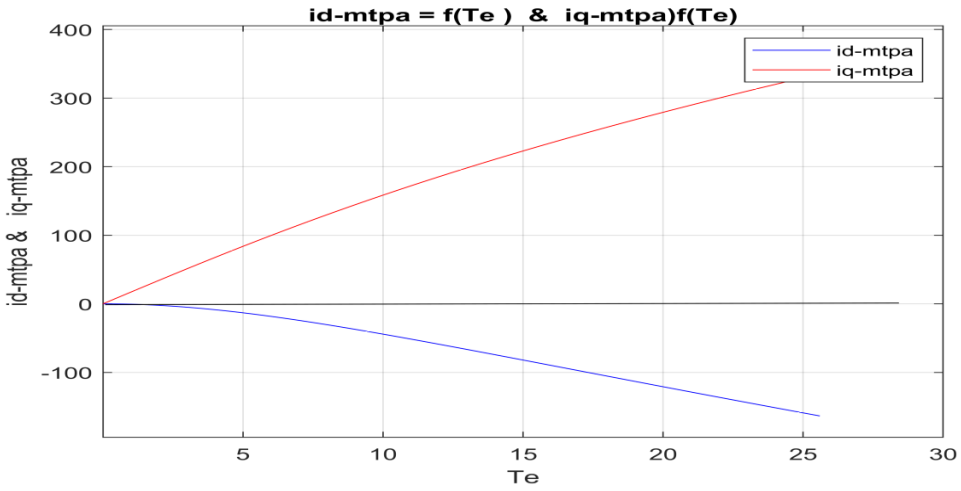

Figure 3-4: - (MTPA curve) Reference currents ($\boldsymbol{i_{d-mtpa}}$ & $\boldsymbol{i_{q-mtpa}}$) Generation from the torque reference

Also, Torque can be calculated from the power output. The output power of a motor sets the speed and torque performance boundaries of a motor, based on the equation:

$$P = (\omega_e * T_e)$$

Where P-Power in watt, ω_e-electrical speed in rpm and T_e- electrical Torque in Nm and v_a, v_b, v_c as the three phase voltages applied to the motor, and i_a, i_b, i_c are the currents strained by the motor. The power supplied to the motor is given by [1], [4], [2].

$P_{abc} = (U_a * i_a + U_b * i_b + U_c * i_c)$ [30]

We can rewrite in matrix form that helps of changed the equation in to $dq - axes$ easily

$$P_{abc} = [i_a \;\; i_b \;\; i_c] \begin{bmatrix} V_a \\ U_b \\ U_c \end{bmatrix} = I_{abc}^t * U_{abc} \text{ [31]}$$

Now we represent the Power in dq-frame

$P_{dqo} = \frac{3}{2}[i_d * e_d + i_q * e_q]$ [32]

The back electromotive force values, e_d and e_q, are given by $e_d = -\omega_e \lambda_q$ and $e_q = \omega_e \lambda_d$. The flux linkage values are $\lambda_d = \lambda_{pm} + L_d i_d$ and $\lambda_q = L_q i_q$, as seen in the field weakening algorithm. The rated output power of a motor is fixed, so speed and torque are inversely related. As speed increases, torque decreases, and vice versa [29]. This relationship is typically shown on a motor performance curve, which also includes motor current (in Amps) and efficiency (%).

3.3 Wide Range Speed Control (Field-Weakening Control)

Wide Range Speed Control for an Interior Permanent Magnet Synchronous Motor (IPMSM) extends the motor's speed range by controlling both torque and flux. In Field Weakening Control (FWC), the motor operates above rated speed by reducing magnetic flux to maintain constant torque while keeping current within safe limits.

When using the Field-Oriented Control (FOC) algorithm with rated flux, the maximum speed is limited by stator voltages, current, and back EMF (base speed). Above this speed, back EMF exceeds supply voltage. Setting a negative d-axis current reduces rotor flux, enabling operation beyond base speed. This is field-weakening control [3].

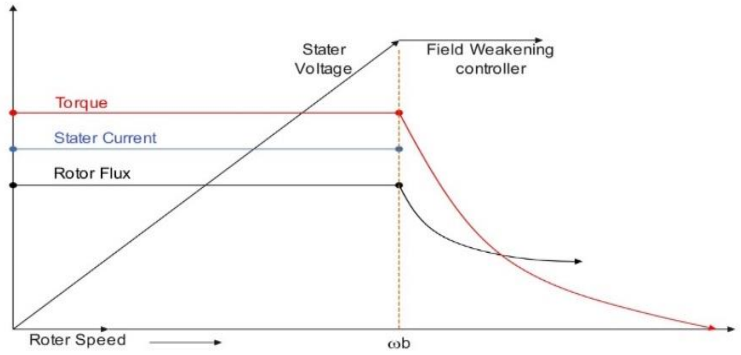

Figure 3-5: - shows MTPA and Wide Speed Range (Field Weakening) positions

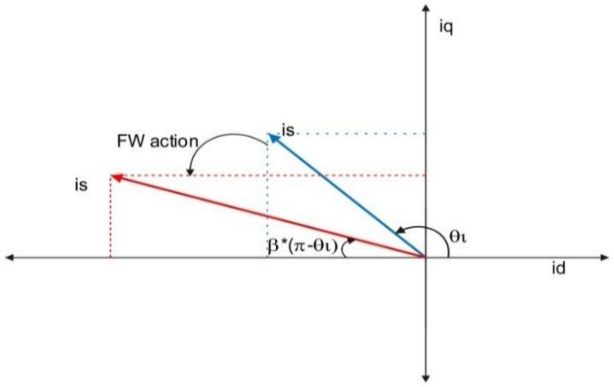

Figure 3-6: - Field Weakening action of the implemented control

Wide Speed Control (Field Weakening) Algorithm

The speed of the IPMSM is regulated using indirect Field-Oriented Control (FOC). During operation, both current and voltage are maintained below their respective limits. These constraints are determined by the inverter's maximum current and the DC link's maximum available voltage. Mathematically, these limits can be expressed as follows::

$$i_d^2 + i_q^2 = i_{mux}^2$$
$$U_d^2 + U_q^2 = U_{mux}^2 \leq Udc \qquad 3.46$$

U_{max} the inverter's maximum phase-voltage amplitude The steady state dq voltage equations can be expressed using the $dq - flux$ dynamic voltage equations of the IPMSM and the dq-flux equations that were introduced in Unit 2.

Steady-State Equations for IPMSM

In steady-state operation, the IPMSM can be modeled using the following equations:
Voltage Equations [6]:- In the rotor reference frame (d-q frame), the voltage equations for the stator are given as:

$$U_q = R_s i_q - \omega_e * L_q i_q,\ (R_s = 0)\ \rightarrow U_q = -\omega_e L_q i_q$$
$$U_d = R_s i_d + \omega_e L_d i_d + \omega_e \lambda_{pm},\ (R_s = 0) \rightarrow U_d = \omega_e (L_d i_d + \lambda_{pm}) \quad 3.47$$

The stator resistance is neglected, by substituting the d and q voltage equations in the steady state dq voltage equations constraint.
In Field Weakening mode, the current i_d becomes non-zero and is used to reduce the effective flux, thereby allowing the motor to operate at higher speeds without exceeding the voltage limits.

Wide Speed Control in Transient State

In the transient state, the system must consider both the dynamics of the motor and the controller response. The control algorithm typically involves managing the voltage limits while transitioning from normal operation to field weakening [2]. The dynamic equations during transient operation are:

$$u_{qs} = R_s i_q + \frac{\partial}{\partial t}\lambda_q - \omega_e \lambda_d$$
$$u_{ds} = R_s i_d + \frac{\partial}{\partial t}\lambda_d - \omega_e\, \lambda_q \quad 3.48$$

Substitute the Upper equation ($\lambda_q = L_q i_q$) and ($\lambda_d = (L_d i_d + \lambda_{pm})$ it gives

$$u_q = R_s i_q + \frac{\partial}{\partial t}(L_q i_q) - \omega_r L_d i_d$$
$$u_d = R_s i_d + \frac{\partial}{\partial t}(L_d i_d + \lambda_{pm}) - \omega L_q i_q \quad 3.49$$

And eliminate the value of R_s and the stady state equation for controlling mechanism we get the transient state equation as follow: -

$$u_q = L_q \frac{\partial}{\partial t}(i_q) - \omega_r L_d i_d \rightarrow u_q = L_q \frac{d}{dt}(i_q)$$
$$u_d = L_d \frac{\partial}{\partial t}(i_d) - \omega L_q i_q \rightarrow u_d = L_d \frac{d}{dt}(i_d) \quad 3.50$$

The control system must dynamically adjust the reference currents i_d and i_q to ensure that the motor operates in the desired speed range while avoiding over-voltage. The transient process also needs to account for the controller's bandwidth, which limits the rate at

which the current and flux can change [30]. For control, the Transient State equations are applied with an IP controller for current control as show on the following: -

$$i_d = K_p * (i_{dref} - i_{dmeas}) + K_i * \int (i_{dref} - i_{dmeas})dt$$
$$i_q = K_p * (i_{qref} - i_{qmeas}) + K_i * \int (i_{qref} - i_{qmeas})dt \quad 3.51$$

This framework ensures steady-state and transient control for an IPMSM under Field Weakening (FWC). Effective FWC involves managing the d-axis current (i_d) relative to motor speed for desired performance while maintaining stability. A PI controller and voltage saturation algorithm is used for current control, ensuring the motor operates within voltage limits. The voltage saturation is modeled by $\boldsymbol{U_q^2 + U_d^2 = U_{max}^2}$ where this was better than or equal to the rated voltage.

- **Steady-State Field Weakening**: -Achieved by reducing i_d to decrease back EMF and enable operation above rated speed.
- **Transient State Field Weakening**: -Manages voltage and current dynamically to prevent exceeding voltage limits while transitioning between normal and field weakening modes. This control is crucial for high-speed applications, ensuring balance between magnetic field and applied voltage.

Arrangement of Wide speed Range speed control strategy

Wide speed range (Field Weakening) control reduces the motor's back EMF by inserting a negative i_d current component, limiting the total voltage to the motor's maximum voltage U_{max}. The flux is controlled by adjusting i_d, with the goal of keeping the stator voltage within the motor's rated limit. In Field Weakening, the motor's flux is reduced through ($\lambda_d = \lambda_{pm} + L_d * i_d$ and $\lambda_q = L_q * i_q$), while the torque T_e control adjusts i_q. The maximum voltage constraint is given by $U_{max} = \sqrt{(U_q^2 + U_d^2)} \leq U_{rated}$. To avoid above this limit, U_d is typically controlled to be negative, and i_d is adjusted to maintain flux reduction.

For wide-speed range operation, the voltage constraint is

$$U\_max \geq \sqrt{((R\_s * i\_d)^2 + (\omega\_e * L\_q * i\_d)^2 + (\omega\_e * \lambda\_pm)^2)} \quad 2.5\ [12]$$

When the motor exceeds the rated voltage, speed increases with higher voltage or flux reduction. In the high-speed range, voltage cannot be increased further, and flux reduction via Field Weakening is required. The optimum operating point for torque and speed is determined by the intersection of the torque trajectory and the voltage

limit ellipse in the i_d, i_q plane. The voltage is constrained, and the back EMF increases with speed, so above base speed, the flux needs to be decreased to avoid exceeding the voltage limits $\boldsymbol{\lambda_{pm}} = \frac{U_{max}}{\boldsymbol{\omega_e}}$ [12]. In this case, the control strategy shifts from the MTPA to Field Weakening Control. This proposed in [20] is to minimize the total electrical loss under the voltage limit. For a given requirement (W_e , T_e), the intersection of the torque trajectory curve and voltage limit ellipse in the i_d, i_q plane is the optimum operating point in this situation.

If the stator resistance is neglected, by substituting the U_d and U_q voltage equations in thesteady state U_{dq} voltage equations constraint

$$\begin{aligned} U_q &= -\omega_e L_q i_q \\ U_d &= \omega_e (L_d i_d + \lambda_{pm}) \\ U_{DC}^2 &= U_q^2 + U_d^2 \end{aligned} \qquad 3.52$$

and Substitute the value of U_{dq} voltages the U_DC became

$$\boldsymbol{U_{DC}^2 = -\omega_e^2 \lambda_q^2 + \omega_e^2 (\lambda_d + \lambda_{pm})^2} \qquad 3.53$$

Divided both side by ω_e^2

$$\frac{U_{DC}^2}{\omega_e^2} = -\lambda_q^2 + (\lambda_d + \lambda_{pm})^2 \qquad 3.54$$

Then substitute the value of U_{max} in the equation (2.67) finally we get

$$\left(\frac{\boldsymbol{U_{max}}}{\omega_e}\right)^2 \geq L_d^2 * \left(\frac{\boldsymbol{\lambda_{pm}}}{L_d} + i_d\right)^2 + (L_q * i_q)^2 \qquad 3.55$$

The ellipse, centered at $linf = (-\frac{\lambda_{pm}}{L_d}, 0)$, represents the voltage limit in the current i_d, i_q plane. This center is the "infinite speed point," where the motor speed is theoretically infinite. As motor speed (ω_e) increases, the ellipse radius decreases toward the center. The ellipse equation (voltage limit) and the circle equation $i_d^2 + i_q^2 = i_{max}^2$ (current limit) together define the constraints in the i_d, i_q plane for an IPMSM, as shown in the Figure.

Equating equation (2.67) with zero to find the value of i_q and i_d current

$$\boldsymbol{(L_d^2 - L_q^2) i_d^2 + 2\lambda_{pm} L_d i_d + \lambda_{pm}^2 L_q^2 I_a^2 - \frac{u_{DC}^2}{\omega_e^2} = 0} \qquad 3.56$$

This equation describes the computation field weakening current of maximum possible torque corresponding to a given speed value by using quadratic equation formula $\frac{-b\pm\sqrt{b^2-4ac}}{2a}$ we can drive the value of i_{d-FW}

$$i_{d-FW}=\left[\frac{-\lambda_{pm}L_d\pm\sqrt{(\lambda_{pm}L_d)^2-\left(\left(L_d^2-L_q^2\right)\right)\left(\lambda_{pm}^2L_q^2I_a^2-\frac{u_{DC}^2}{\omega_e^2}\right)}}{\left(L_d^2-L_q^2\right)}\right] \quad 3.57$$

Then also calculate the value of current i_{d-FW} is as follow

$$i_{q-FW}=\sqrt{I_a^2-i_{d-FW}^2} \quad 3.58$$

The following two equation describe computation of field weakening current from the given speed and torque the value of i_q becomes: -

$$i_{q-FW}=\frac{\lambda_{pm}}{L_d}+\frac{1}{L_d}\sqrt{\frac{u_{DC}^2}{\omega_e^2}-i_{d-FW}^2} \quad 3.59$$

The Electrical Torque of motor is

$$T_e=\left[\left(\frac{3P}{4}(\lambda_{pm})i_{q-FW}\right)^2+\left(\frac{3P}{4}(L_d-L_q)(i_{q-FW}*i_{d-FW})\right)^2\right] \quad 3.60$$

To decrease computation time, the system approximates the polynomial solution. For negative reference torque, the signs of I_a and $I\_(q-ref)$ are updated and equations are adjusted. The terminal voltage difference created by the operation region is defined by $\frac{1}{\sqrt{3}}-\frac{\sqrt{U_d^2+U_q^2}}{U_{dc}}\geq 0$ (constant torque, MTPA area) $\frac{1}{\sqrt{3}}-\frac{\sqrt{U_d^2+U_q^2}}{U_{dc}}\leq 0$ (constant power, Field Weakening area). The wide-speed-range (FW) controller is an integrator with anti-windup. It measures U_{dq} voltages and the DC-link voltage to analyze the modulation index (M) using: $M=\frac{\sqrt{U_d^2+U_q^2}}{U\_dc}$ [9]. The error between measured and threshold M is fed to the integrator. The output (Bc), limited between 0 and 1, adjusts the stator current angle. If the error is positive, $Bc=1$ (no change in current angle). If negative $Bc=-1$, Bc decreases, dropped the stator current angle and activating field weakening [3]. The pictorially representation of the FW action, is presented in Figure.

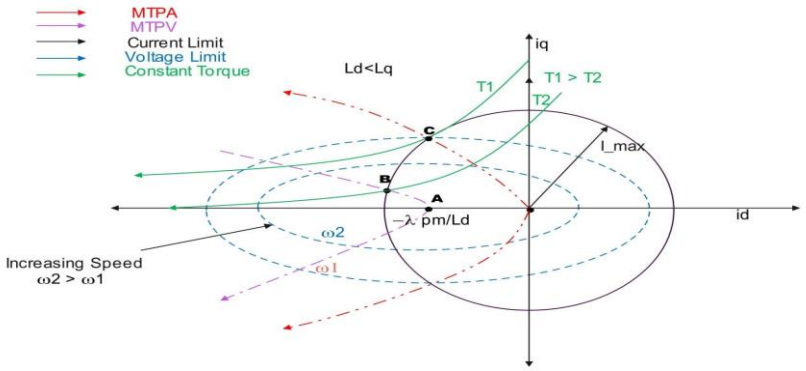

Figure 3-7: - i_d *amd* i_q representation of the voltage and current limitation

Field Weakening (FW) control First, a reference modulation index (M_{ref}) is set. The current regulators (PI controllers for i_d and i\sub>q</sub>) may be saturated in FW mode, which could lead to a loss of motor control because of voltage restrictions. Potential saturation is indicated as the modulation index (M) approaches 1. The FW algorithm establishes a threshold just below 1 to avoid this and ensure steady operation. [5], [31]. When the modulation index decreases below the threshold (due to reduced load or speed), the integrator output rises to 1, exiting FW mode. The FW control principle, shown in Figure 2-8, involves calculating θ (from $-\frac{\pi}{2}$ to 0) based on the difference between $\frac{1}{\sqrt{3}}$ and $\frac{\sqrt{U_d^2 + U_q^2}}{U_{dc}}$ through the PI controller. In FW mode, θ is negative and used to adjusti_q.. $\left(i_q = \mid i_q \mid * \ sin(\theta)\right)$, which results in a reduced dq_{axis} current (i_{d-fw} and i_{q-fw}), allowing speed (ω_e) to increase as dq_{axis} current decreases [5], [32].

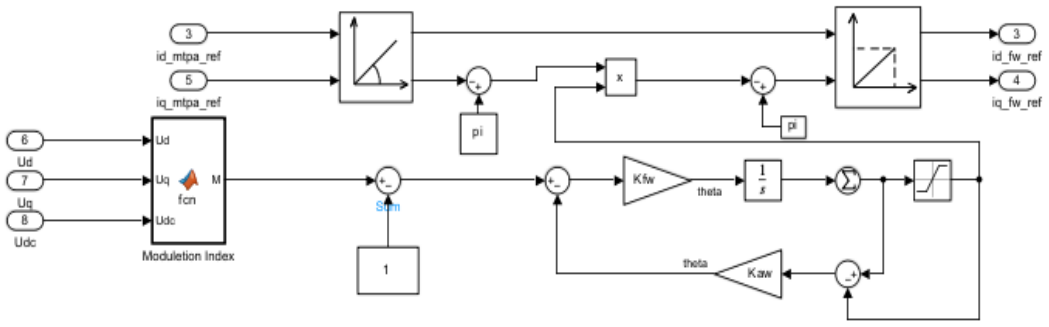

*Figure 3-8: -*Field Weakening block diagram on MATLAB simulation

3.4 Current Control Tuning

Since higher-level mechanical loops, such speed and position control, rely on the present control loop's optimal performance, it is essential to the vector control system's

architecture. The system can quickly track reference currents from the speed controller by using this inner loop, which guarantees excellent dynamic performance even in the event of sudden changes in position or speed. Furthermore, the current loop permits decoupled control of the torque-producing and magnetizing components while maintaining current within safe bounds. components id and iq. The main reason why the stator current must not exceed its maximum is the demagnetization of permanent magnets of the machine. The design of the current controllers for d-axis and q-axis assumes that current changes are much faster than mechanical changes. The behaviour of the circuit is described by equation (4-1), which can be rewritten in the frequency domain in the form.

$$\boldsymbol{U_{dq} = Gi_{dq} * Wi_{dq} + E}$$

$$\boldsymbol{G} = \begin{bmatrix} \dfrac{1}{R_s + sL_d} & 0 \\ 0 & \dfrac{1}{R_s + sL_q} \end{bmatrix}, \qquad \boldsymbol{E} = \begin{bmatrix} o \\ \lambda_{pm} \end{bmatrix}$$

$$\begin{bmatrix} U_d \\ U_q \end{bmatrix} = \begin{bmatrix} L_d \\ L_q \end{bmatrix} * \frac{d}{dt} \begin{bmatrix} i_d \\ i_q \end{bmatrix} + \begin{bmatrix} R_s & -\omega_r L_q \\ \omega_r L_d & R_s \end{bmatrix} * \begin{bmatrix} i_d \\ i_q \end{bmatrix} + \omega_r \begin{bmatrix} o \\ \lambda_{pm} \end{bmatrix} \qquad 3.36$$

$$\boldsymbol{L_d = L_s - \Delta L_s \, , L_q = L_s + \Delta L_s}$$

$$T_e = \frac{3P}{2}\left[(\lambda_{pm})i_q + (L_d - L_q)i_d i_q\right]$$

PI Controller Design on IPMSM

The PI (Proportional-Integral) controller is used in IPMSM (Interior Permanent Magnet Synchronous Motor) to improve system response and reduce errors. Here's a brief outline for designing a PI controller for IPMSM:

To understand System Dynamics is Familiarize with the IPMSM model, including torque, back EMF, and current equations. Set goals such as fast response, stability, and minimizing torque ripple to Define Control Objectives. Control the d-axis (id) and q-axis (iq) currents separately, with iq typically for torque control and id for flux weakening to Select Control Variables**.** Implement a current control structure loop using feedback from motor sensors to process the error between reference and actual currents.

Design the PI Controller: The transfer function for the PI controller is $C(s) = Kp +$ $C(s) = K_p + \frac{K_i}{s}$, where K_p is the proportional gain and K_i is the integral gain. Model

the motor and controller in tools like MATLAB/Simulink to validate performance under various conditions (step responses, disturbances, etc.) under simulation. Implement anti-windup measures for actuator saturation and filtering techniques to reduce noise in current measurements. It includes fault detection and safety mechanisms to protect the motor and drive.

Under Tuning is methods is used to like Ziegler-Nichols, pole placement, or root locus for tuning to ensure the desired transient response (rise time, settling time, overshoot). Feedforward Control (Optional): Add feedforward control to improve response time by predicting the necessary control action based on desired torque and speed. Under this thesis we proposed only the tuning system for the current.

Tuning of PI Current Controller on IPMSM

The current control loop plays a crucial role in vector control design since higher-level mechanical control loops, including those for speed and position, rely on its optimal performance. Even in the event of sudden changes in position or speed, this inner loop guarantees exceptional dynamic response by quickly detecting the reference currents provided by the speed controller. The torque-producing (i_q) and magnetizing (i_d) currents can also be controlled separately thanks to it, as long as the overall current stays within safe operating bounds.

$$U_d = R_s * i_d(s) + sL_d * i_d(s)$$
$$U_q = R_s * i_q(s) + sL_q * i_q(s) \qquad 3.7$$

The given term transfer function of IPMSM of $d\&q$ current. For proportional control we use this equation format

$$P_d(s) = \frac{1}{s * L_d + R_s} = \frac{1}{R_s(sL_d + 1)} = \frac{1}{R_s(s * T_{sd} + 1)}$$
$$P_q(s) = \frac{1}{s * L_q + R_s} = \frac{1}{R_s(sL_q + 1)} = \frac{1}{R_s(s * T_{sq} + 1)} \qquad 3.8$$

$T_{sd} = \frac{L_d}{R_s} = d - electrical\ time\ constant\ and$

$T_{sq} = \frac{L_q}{R_s}\ q - electrical\ time\ constant$

Tuning the $\boldsymbol{i_q}\ and\ \boldsymbol{i_d}$ PI controller

The delay due to the digital controller (control algorism) first order transfer function Time constant equal to

$$U_d = R_s * i_d(s) + sL_d * i_d(s)$$
$$U_q = R_s * i_q(s) + sL_q * i_q(s) \quad 3.9$$

$$T_{sw} = \frac{1}{f_{sw}} = \frac{1}{0.5KHz} = 0.2ms \quad 3.10$$

Modulation index (Invertor) first order transfer function Time constant equal to

$$T_{sw} * 0.5 = 0.1ms$$

Modulation index (Invertor) first order transfer function Time constant equal to

$$T_{sw} * 0.5 = 0.1ms$$

$$PI_q = K_{pq} * \frac{1 + \tau_q s}{\tau_q s} \quad 3.11$$

The i_q current loop can be redrawn to have a unity feedback [27]

The control structure

is represented.

The open loop transfer function of $\boldsymbol{i_q}$ have unit feedback

$$G_{oq} = \left(K_{pq} * \frac{1+\tau_q s}{\tau_q s} * \frac{1}{(0.5*T_{sw}s+1)} * \frac{1}{(T_{sw}s+1)} * \frac{1}{(0.5*T_{sw}s+1)} * \frac{1}{(0.5*T_{sw}s+1)} * \frac{1}{R_s(T_{sq}s+1)} \right) \quad 3.12$$

[1].

Since the zero of the PI transfer function is made to cancel out, the lowest pole—which is one of the PIMSM transfer functions—is provided as

$$\tau_q = \frac{L_q}{Rs} = T_{swq} \quad 3.13$$

To determine the PI controller's gain, all first-order transfer functions that cause delays are roughly

$$T_{si} = (3 * 0.5) * T_{sw} + T_{sw} = 2.5T_{sw}$$
$$T_{si} = (1.5) * T_{sw} + 1T_{sw} = 2.5T_{sw} \quad 3.14$$
$$T_{si} = 2.5T_{sw} = 2.5 * 0.2 = 0.5$$

The equivalent open loop transfer function of IPMSM approximately time constant

$$G_{oq} = \frac{K_{pq}}{\tau_q s} * \frac{1}{R_s(T_{si}s + 1)} \quad 3.15$$

Optimal Modulation

Damping factor are chooses $\boldsymbol{C} = \xi = \frac{\sqrt{2}}{2}$ based on optimal criterion. Open loop second order transfer function system with damping factor Criterion

$$G = \frac{1}{2 * \xi s(1 + \xi s)} \quad 3.16$$

Comparison between The PI controller's open loop transfer function gain and second order transfer function can be

$$\frac{K_{pq}}{R_s * \tau_q} = \frac{1}{2T_{si}} = K_{pq} = \frac{R_s \tau_q}{2T_{si}} \quad 3.17$$

Transfer function of PI controller has

$$PI_q = \frac{KP_q(1 + \tau_q s)}{\tau_q s} \quad 3.18$$

Closed loop PI controller

$$G_{cq} = \frac{1}{2 * T_{si}^2 * S^2 + 2}$$
$$G_{cq} = \frac{1}{2 * T_{si}^2 * S + T_{si} * S + 1} \quad 3.19$$

Transfer function: - after Neglecting the second order time constant is equal to

$$\tau_{iq} = 2T_{si} - 0.5T_s \quad 3.20$$

Tuning of i_d PI controller

To design i_d current it the only difference between the i_q *current loop and the* i_q current is the transfer function of IPMSM, which varies because of the L_d *and* L_q inductance.

The PI's transfer function on the d-loop

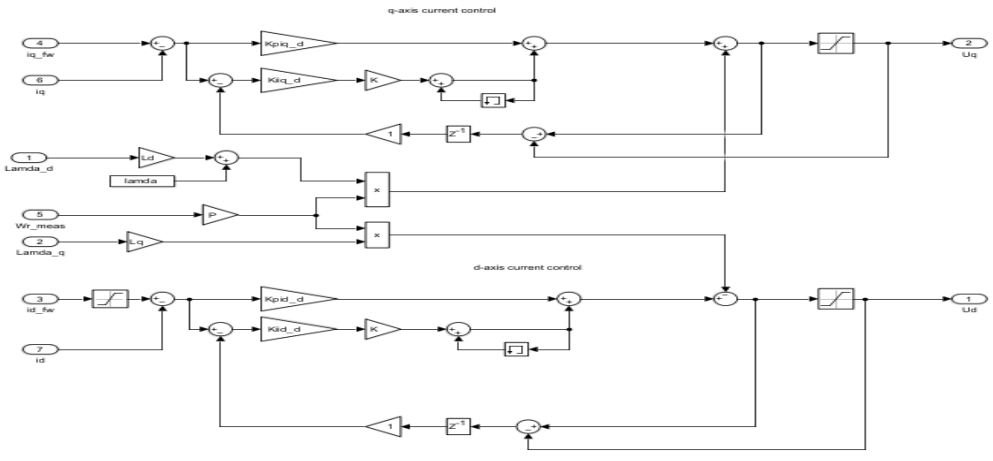

Figure 3-9: - The tuning PI current control with anti-wend up block diagram on MATLAB Simulink

The reference was based on the torque (T_e) generated by SMC and other controllers. This subsystem calculated optimized reference currents (i_d) and (i_q) using field-weakening

methods and MTPA, considering real motor speed, predictable motor characteristics, and supply voltage. The controlled current (shown as a red broken line) was compared with outputs from MTPA and field weakening. Current regulators received (i_{d-ref}) and (i_{q-ref}) to generate reference voltages (U_d) and (U_q), effectively controlling the system. A feed-forward computation of IPMSM currents, based on motor characteristics, was utilized to enhance regulator performance and dynamics [3].

3.5 Space Vector Pulse Width Modulation (SVPWM)

Sinusoidal PWM (SPWM) and Space Vector PWM (SVPWM) are widely used techniques for controlling motor drives. SPWM reduces total harmonic distortion (THD) and is relatively simple to implement. It generates gating signals by comparing a sinusoidal reference with a triangular carrier waveform, with the modulation index (M_s) controlling output voltage amplitude. SPWM can be implemented in either bipolar or unipolar forms.

The modulation index (M_s) is defined as:- $M_s = \frac{V_{controled}}{V_{triangle}}$ The frequency modulation ratio (M_f) is:- $M_f = \frac{f_{triangle}}{f_{control}}$. SVPWM is greater to SPWM, contribution ~15% more output voltage and reduced switching losses. It transforms the $dq - axis$ voltages into the $\alpha\beta$ reference frame.

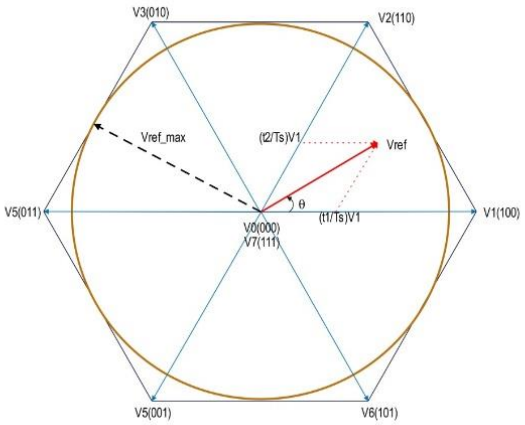

Figure 3-10: - Voltage space vector locations corresponding to different switching states

Using inverse Clarke transformation. The reference voltage vector is positioned within one of six 60° sectors, with active vectors for switching (100, 110, 010, 011, 001, 101) and zero vectors (000, 111). The switching durations are calculated as: -

$$t_1 = M_p * T_s * sin\left(n * \frac{\pi}{3} - \theta\right)$$

$$t_2 = M_p * T_s * sin\left(\theta - (n-1) * \frac{\pi}{3}\right)$$

$$T_0 = T_s - (t_1 + t_2)$$

where $\theta, n, M,$ and T_s are the angle, sector number, modulation index, and sampling time, respectively. The modulation index is: $M_P \frac{\sqrt{3} * V_{ref}}{V_{DC}}$ [33].

The working principle of Space Vector PWM (SVPWM) involves a three-phase inverter that converts DC supply into three-phase output for a motor. The inverter switches are controlled to prevent both switches in the same leg from being on at the same time, avoiding a short circuit. This is achieved through complementary operation: when one switch (e.g., A^+) is on, the other (A^-) is off, and vice versa. This results in eight possible switching vectors (V_0 to V_7), with six active vectors and two zero vectors. The active vectors produce a pulsed sinusoidal output voltage with each leg offset by 120°, SVPWM (Space Vector Pulse Width Modulation) is commonly used in multi-level inverters. It converts three-phase components into two-phase components, representing the system as space vectors in a 2D plane. The transformation allows easier analysis and control of the three-phase system. [33].

3.6 Power Inverter Overview

An inverter converts DC voltage into AC voltage of desired frequency and waveform. It's widely used in renewable energy systems, motor drives, and UPS systems. In motor drives, inverters control the motor's speed and acceleration, expanding the motor's application range by allowing variable speeds.

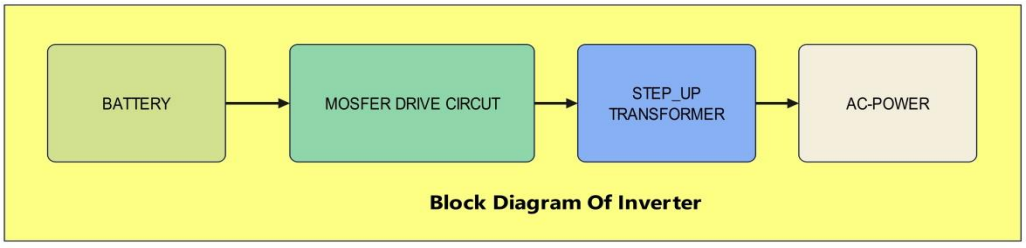

Types of Inverters:

Voltage Source Inverter (VSI): - Uses DC voltage as input, often from batteries or solar panels they are Simpler, more efficient, and widely used and their Types are

Half-bridge (2 switches), Full-bridge (4 switches), and Multilevel (reduces harmonics).

Current Source Inverter (CSI): - Uses DC current as input, used in specialized applications like flexible AC transmission and they are More complex due to design challenges.

An investor is divided also Based on Voltage Output

Two-Level Inverter**,** Simple design with two switches for positive and negative voltages and easy and cost-effective, but generates more harmonics.

Three-Level Inverter, are More advanced, uses three switches and can produce three voltage levels (positive, zero, and negative) and also, they deliver smoother, more sinusoidal output, ideal for sensitive loads and can produce higher voltage.

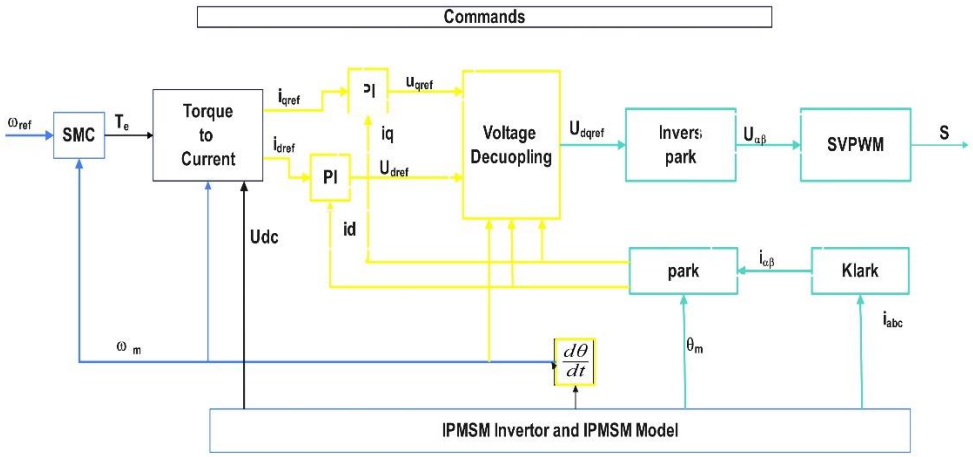

Figure 3-11: - shows block diagram for control structure of IPMSM

CHAPTER 4

4 Interior Permanent Magnet Synchronous Motor Controller Designing

4.1 Introduction

The general block diagram of the vector control system includes core components such as PI controllers, reference current generation, and both speed and first-order sliding mode controllers. The control structure relies on a series of coordinate transformations—Clarke, Park, and inverse Park—to transition between stationary and rotating reference frames. Additionally, Space Vector Pulse Width Modulation (SVPWM) is employed to determine inverter gate timing based on the controlled d–q axis voltage vectors, ensuring the proper voltage is applied to the stator windings. By using feedback from measured stator currents and rotor speed, the controller accurately regulates the machine to follow the desired setpoints.

4.2 Sliding Mode Control (SMC) Designing on IPMSM

The first step in designing an SMC is to define the sliding surface. A common choice is based on the speed error between the desired speed W_{e-ref} and the actual speed W_e. Define the error as:

$$\frac{dW_e}{dt} = \frac{P}{J}(T_e - T_l - B\,W_e) \qquad 4.1$$

Where: $W_e -$ is the actual speed,$P -$ is a system parameter., $J -$ is the moment of inertia,

$T_e -$ is the control input (electromagnetic torque), $T_l -$ is the load torque (disturbance), $B -$ is the damping coefficient., $W_{e-ref} -$ is the reference Speed, $e -$ is the tracking error

$$e = W_e - W_{e-ref} \qquad 4.2$$

From the Binging we start to define the Sliding Surface, In SMC, the sliding surface (S) is designed to include SMC. Let the sliding surface be define the sliding surface S

$$S = e + C \int e\, dt \tag{4.3}$$

Where:

$C > 0$ is a design parameter.

Derivative the Sliding Surface S

Take the derivative of S: -

$$\frac{dS}{dt} = \left(\frac{de}{dt} + C\, e\right) \tag{4.4}$$

Substitute the value of error presentation $\frac{de}{dt} = \left(\frac{dW_e}{dt} - \frac{dW_{e-ref}}{dt}\right)$,

$$\frac{dS}{dt} = \frac{P}{J}\,(T_e - T_l - B\, W_r) - \frac{dW_{e-ref}}{dt} + C\, e \tag{4.5}$$

To design the sliding Control Law of electrical torque (T_e) is designed to confirm that the system reaches the sliding surface S = 0 and remains on it. The control law covers two parts:

1. Equivalent Control T_{e-eq} : Confirms $\frac{dS}{dt} = 0$ in the absence of disturbances.
2. Switching Control T_{e-sw} : Compensates for uncertainties and disturbances.

The total control input is

$$T_e = T_{e-eq} + T_{e-sw} \tag{4.6}$$

Equivalent Control T_{e-eq}

Set $\frac{dS}{dt} = 0$ and solve for T_{e-eq}

$$\begin{aligned} 0 &= \frac{P}{J}\left(T_{e-eq} - T_l - BW_e\right) - \frac{dW_{e-ref}}{dt} + Ce \\ T_{eq} &= T_l + B\, W_e + \frac{J}{P}\left(\frac{dW_{e-ref}}{dt} - Ce\right) \end{aligned} \tag{4.7}$$

Switching Control T_{e-sw}

The switching control is designed to ensure reachability of the sliding surface:

$$T_{e-sw} = \frac{J}{P} K sign(S) \tag{4.8}$$

Where: K is a gain parameter, $sign(S)$ is the signum function.

Finally, the sliding mode Control Law is combining $T_{e-eq} + T_{e-sw}$, the total control input is:

$$T_e = T_l + B\,W_e + \frac{J}{P}\left(\frac{dW_{e-ref}}{dt} - C\,e\right) - \frac{J}{P}Ksign(S) \qquad 4.9$$

Stability Analysis

For the sliding mode stability analysis is used to confirm that stability of the system that we used Lyapunov function.

$$V = \frac{1}{2}(S^2) \qquad 4.10$$

We used the derivative of the Lyapunov function is:

$$\frac{dV}{dt} = S * \frac{dS}{dt} \qquad 4.11$$

Substitute $\frac{dS}{dt}$ in to the upper equation

$$\frac{dV}{dt} = S((T_e - T_l - B\,W_e) - \frac{dW_{e-ref}}{dt} + Ce) \qquad 4.12$$

Substitute the electrical torque in to the equation (T_e)

$$\frac{dV}{dt} = S(\frac{P}{J}\frac{dV}{dt} = S\frac{P}{J}\Big(\Big(T_l + B\,W_r + \frac{J}{P}\Big(\frac{dW_{e-ref}}{dt} - C\,e\Big) - \frac{J}{P}Ksig(S)) - T_l - B\,W_e\Big) - \frac{dW_{e-ref}}{dt} + C\,e\Big) \qquad 4.13$$

$$\frac{dV}{dt} = S\big(-Ksign(S)\big)$$
$$\frac{dV}{dt} = -K|\,(S)\,| \qquad 4.14$$

$\frac{dV}{dt} \leq 0$ is the system being stable and the sliding surface $S = 0$ is reached infinite time.

In general, the sliding mode control low is becoming: -

$$T_e = T_l + B\,W_e + \frac{J}{P}\left(\frac{dW_{e-ref}}{dt} - Ce\right) - \frac{J}{P}Ksign(S)$$
$$T_e = T_l + B\,W_e + \frac{J}{P} - Ce - \frac{J}{P}Ksign(S) \quad (4.15)$$

The Lyapunov stability analysis confirms that the system will converge to the sliding surface and remain there, ensuring stability. The designed Sliding Mode Control law drives the system to the desired state and guarantees asymptotic stability

4.3 Designing Integral Sliding Mode Control (I-SMC)

The goal of designing an Integral Sliding Mode Control (ISMC) for the speed equation is to combine the benefits of sliding mode control with integral action to recover system performance, particularly steady state error in tracking and disturbance rejection, while ensuring stability using Lyapunov's method.

Let's break down the steps for the Integral Sliding Mode Control of the speed equation of Interior PMSM.

$$\frac{dW_e}{dt} = \left(\frac{P}{J}\right) * (T_e - T_l - BW_e) \quad (4.16)$$

Express the error that created by reference speed and actual speed

$$e_1 = W_{e-ref} - W_e$$
$$e_2 = \dot{e_1} = -\dot{W}_e \quad (4.17)$$
$$\dot{e_1} = \frac{dW_{e-ref}}{dt} - \frac{dW_e}{dt}$$

From the motion equation we can drive the equation

$$\frac{dW_e}{dt} = \left(\frac{P}{J}\right) * (T_e - T_l - BW_e)$$
$$e_2 = \dot{e_1} = -\dot{W}_e \quad (4.18)$$
$$\dot{e_1} = -W_e = \left(\frac{P}{J}\right) * (T_e - T_l - BWe)$$

The time derivative of $\dot{e_1}$ is becomes

$$\ddot{e_1} = \dot{e_2}$$
$$\dot{e_2} = \ddot{W_e}$$
$$\dot{e_2} = \ddot{e_1} = \frac{P}{J}\left(\dot{T_e} - B\dot{W_e}\right) = -\frac{B}{J}(x_2) - \frac{P}{J}(\dot{T_e}) \qquad 4.19$$

To progress the system, an **integral error term** is presented. Define the integral error as follow:

$$e_{intg} = \int_0^t e(\tau)d\tau \qquad 4.20$$

The sliding surface switching function is chosen from ISMC. Designing the Sliding Surface- The sliding surface is defined to achieve desired system behaviour. The state of the system is designed to reach and stay on this surface.

$$S(e, e_{intg}) = Ce + Ce_{intg} + \dot{e_1}$$
$$S = Ce + Ce_{intg} + \dot{e_1} \qquad 4.21$$
$$C = Ce_1 + e_2$$

Where: $\boldsymbol{C}$ **is** positive constants that control the comparative importance of the tracking error and its integral. This sliding surface confirms that the system stays on the surface and drives the error to zero,

The time derivative of the integral sliding surface switching function becomes

$$\dot{S}\left(e, e_{intg}\right) = (C\dot{e} + C\dot{e}_{intg} + \ddot{e_1}) \qquad 4.22 \text{ A}$$
$$\dot{S} = C\dot{e} + C\dot{e}_{intg} + \dot{e_2} \qquad \text{B}$$
$$\dot{S} = C\dot{e_1} + \ddot{e_1} \qquad \text{C}$$
$$\dot{S} = Ce_2 - \frac{B}{J}e_2 - \frac{P}{J}(\dot{T_e}) \qquad \text{D}$$
$$\text{E}$$

Since $\dot{e_1} = \frac{dW_{e-ref}}{dt} - \frac{dW_e}{dt}$ and typically $\frac{dW_{e-ref}}{dt}$ is constant or zero for a constant reference speed, we get:

$$C\left(\frac{P}{J}(\boldsymbol{T_e} - \boldsymbol{T_l} - \boldsymbol{BW_e})\right) + C\dot{e_1} + \boldsymbol{\ddot{e_1}} \qquad 4.23$$

The exponential reaching low of sliding mode control states that the selected switching

$$\dot{S} = -Ksign\left(S\left(e, e_{intg}\right)\right) - \beta S \qquad 4.24$$

To design the controller there is an input to control T_e designed to drive the system to the sliding surface. In **Integral Sliding Mode Control**,

$$T_e = \dot{T}_e + Ksign\left(S(e, e_{intg})\right) \quad 4.25$$

Combining these two equations and substituting the value of S we get the following equation

$$\dot{S} = \dot{S}$$
$$\dot{S}(e, e_{intg}) = (C\dot{e} + C\dot{e}_{intg} + \ddot{e}) \quad 4.26$$

$$-Ksign\left(S(e, e_{intg})\right) - \beta S = Ce_2 - \frac{B}{J}e_2 - \frac{P}{J}(\dot{T}_e) \quad 4.27$$

$$-Ksign\left(S(e, e_{intg})\right) - \beta(Ce_1 + e_2) = Ce_2 - \frac{B}{J}e_2 - \frac{P}{J}(\dot{T}_e) \quad 4.28$$

$$0 = -Ksign\left(S(e, e_{intg})\right) - \beta Ce_1 + \beta e_2 - Ce_2 - \frac{B}{J}e_2 - \frac{P}{J}(\dot{T}_e) \quad 4.29$$

$$\frac{P}{J}(\dot{T}_e) = Ksign\left(S(e, e_{intg})\right) - \beta Ce_1 + \beta e_2 - Ce_2 - \frac{B}{J}e_2 \quad 4.30$$

$$\dot{T}_e = \frac{J}{P}(Ksign\left(S(e, e_{intg})\right) - \beta Ce_1 + \beta e_2 - Ce_2 - \frac{B}{J}e_2) \quad 4.31$$

$$\dot{T}_e = \frac{J}{P}((\frac{B}{J} - \beta - C)e_2 - \beta Ce_1 - Ksign\left(S(e_1, e_{intg})\right) \quad 4.32$$

Substitute the value of e_1 & e_2

$$\dot{T}_e = \frac{J}{P}\left(\left(\frac{B}{J} - \beta - C\right) * (-\dot{W}_e) - \beta C(W_{eref} - W_e) - KsignS(e, e_{intg})\right) \quad 4.33$$

$$T_e = \int \left(\frac{J}{P}\left(\left(\frac{B}{J} - \beta - C\right) * (-\dot{W}_e) - \beta C(W_{eref} - W_e) - Ksign(S)\right)\right) \quad 4.34$$

$$T_e = \frac{J}{P} * \int \left(\left(\left(\frac{B}{J} - \beta - C\right) * (-\dot{W}_e) - \beta C(W_{eref} - W_e) - Ksign(S)\right)\right)$$

$$T_e = \frac{J}{P}\left(\left(\frac{B}{J} - \beta - C\right) * (-W_e)\right) - \frac{J}{P}(\int \beta C(W_{eref} - W_e)) - \frac{J}{P}(K \int sign(S)) \quad 4.35$$

$$T_e = \frac{J}{P}\left(\left(\frac{B}{J} - \beta - C\right) * (-W_e) - \int \beta C(W_{eref} - W_e) - K \int sign(S)\right) \quad 4.36$$

$\dot{T}_e$ ….*is a control input of the systome*

$$\text{Let } U = \dot{T}_e, \quad -\frac{P}{J} \quad 4.37$$

For Lyapunov's stability check

The sliding mode surface is Designed as $S = Ce_1 + \dot{e_1}$ where C is must be Hurwitz condition $C > 0$

Let $S(e, e_{intg}) = S$ and $V(e, e_{intg}) = V$

The Lyapunov Function Designed as follow: -

$$V = S\dot{S} = \frac{1}{2}S^2$$

$$V(e, e_{intg}) = \frac{1}{2}e_1^2 + \gamma e_{1_{\text{intg}}}^2 \quad 4.38$$

$$V = S\dot{S} = S(C\dot{e_1} + C\dot{e}_{1_{intg}} + \ddot{e}_1) \quad 4.39$$

$$V = S(C\dot{e_1} + C\dot{e}_{1_{intg}} - BU) \quad 4.40$$

According to the Lyapunov stability criteria V is positive definite and it has a continuous First order partial derivative as well as its first order partial derivative is negative semi- definite then the system is stable. In order to ensure that the Lyapunov

$$\dot{T_e} = \frac{J}{P}\left(\left(\frac{B}{J} - \beta - C\right) * (-\dot{W_e}) - \beta C(W_{eref} - W_e) - KsignS(e, e_{intg})\right)$$

$$V = S\dot{S} < 0 \quad 4.41$$

The Integral sliding mode designed as: -

$$\dot{V} = S\dot{S} = S(C\dot{e_1} + C\dot{e}_{1_{intg}} - (-\frac{P}{J})U) \quad 4.42$$

Substituting the value of $-\frac{P}{J}$ and the controller U and combine

$$V = S\dot{S} \quad 4.43$$

$$\dot{V} = S(C\dot{e_1} + C\dot{e}_{1_{intg}} - (-\tfrac{P}{J})U) \quad 4.44$$

$$\dot{V} = S\left[\left(C\dot{e_1} + C\dot{e}_{1_{intg}} - (-\tfrac{P}{J})\dot{U}\right)\right] \quad 4.45$$

$$\dot{V} = S\left[\left(C\dot{e_1} - B * \frac{1}{B}\left((Ke_1 sign(S) - \beta Ce_1 + \beta\dot{e_1} - C\dot{e_1} + C\dot{e}_{1_{intg}})\right)\right)\right] \quad 4.46$$

$$\dot{V} = S(-(Ksign(S) - \beta Ce_1 + \beta\dot{e_1})) \quad 4.47$$

$$\dot{V} = S(-(K)e_1 sign(S) - \beta(S))) \quad 4.48$$

$$V = -(K)S * sign(S) - \beta(S^2) \quad 4.49$$

$$\dot{V} = -(K)\,|\,S\,| - \beta(S^2) \quad 4.50$$

$$\dot{V}(e, e_{intg}) =< -K|\,S(e, e_{intg})\,| - \beta(S^2)$$

This design will drive the speed error $\boldsymbol{e}$ to zero while maintaining robustness against disturbances and uncertainties in the system.

Where $K > 0$ is a positive constant. This negative derivative ensures that $V(e, e_{intg})$ | decreases over time, representing that the system will finally reach the sliding surface

and remain on it. The Integral Sliding Mode Control law for the system can be short as the following: -

$$T_e = T_l + BW_e + \frac{J}{P}\left(Ce + \dot{e} + Ce_{entg}\right) + Ksign\left(S\left(e, e_{intg}\right)\right)$$
$$T_e = \int\left((\beta S + abs(e) * Ksign(S) + C\dot{e}) * \frac{J}{P}\right) \quad 4.51$$

Where: $S\left(e, e_{intg}\right) = Ce + Ce_{entg} + \dot{e}$ is sliding surface, K is a positive gain, λ *and* μ are design parameter for the sliding surface

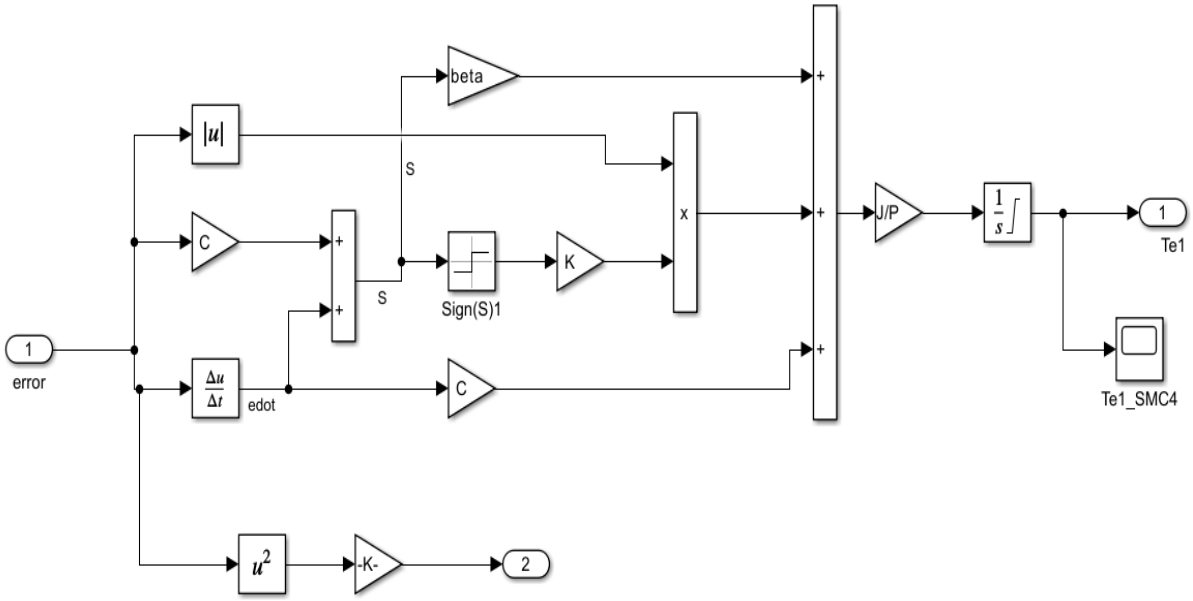

Figure 4-1: - SMC controller design using MATLAB Simulink bock diagram

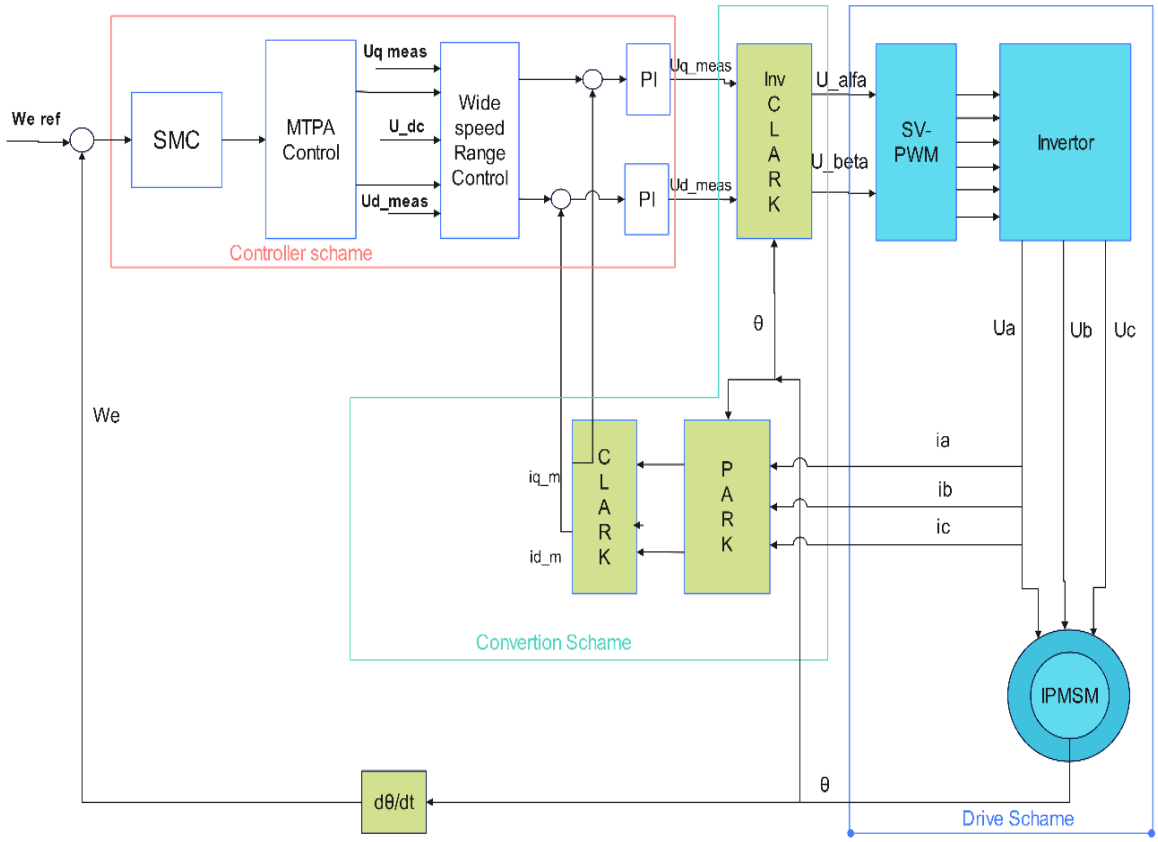

Figure 4-2: - shows block diagram for general structure of MTPA and field-oriented control of IPMSM

CHAPTER 5

5 Simulation Results and Discussion

We are defined deferent explanation that get on the simulation results we prepare it. Now we starting normal mode and generating MTPA mode and field Weakening control. This block diagram shows that all control diagram of the Thesis that include all controlling.

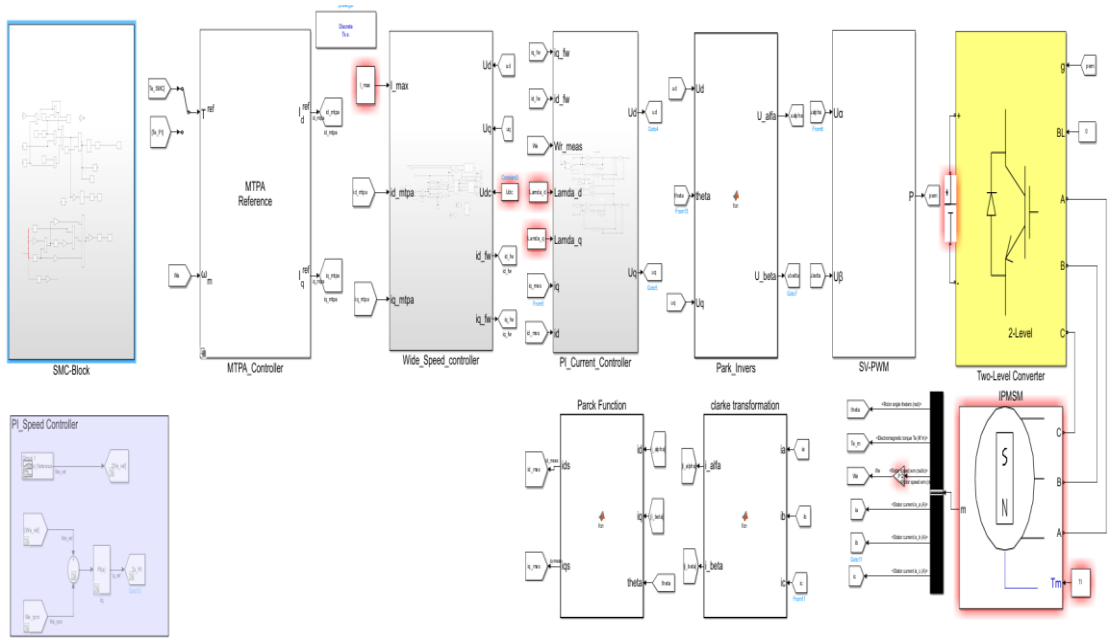

Figure 5-1: Block diagram of Speed Control of IPMSM control Using MTPA and Wide Speed control with SMC

This model has characteristics behavior and specifying the changes in Speed. Under the characteristics change MTPA works up to Base speed (1225) and wide range speed works up to maximum speed (2500) and changing in speed when the motor runs at MTPA current output speed (314 rpm) and in over-speed mode that has wide speed current of 628 rpm as a reference speed. This allows for a pure imagining of system performance and highlights any differences between the two operating modes (MPTA and Wide speed range call it Field Oriented Control FOC) and in addition it includes the reversal speed. At 3.0s, a load torque of 300 N-m was applied to the motor as shown in the figure and after 3-5s, the drive speed increased to 628 rpm and the load torque decreased to 150 N m, after Wide speed range control the speed decrease to -314 rpm at the time of 5-7.0s that indicates the system works in reversal direction and braking mode. The speed manager could handle both speed settings successfully, as shown in the figures.

5.1 Simulation and Desiccation Verification of Speed Control Vs Others

In an Interior Permanent Magnet Synchronous Motor (IPMSM), the relationship between Electrical Torque and Electrical Speed is critical for understanding its performance and relationship can be influenced by several factors, including the motor's design, control method, and operating conditions.

5.1.1 Characteristics curve of IPMSM on Speed vs Torque, Power, Voltage and Current

Electrical Torque and Electrical Speed characteristic curve of an IPMSM have three regions constant torque region, constant power region and field weakening region and their characteristic are: -

Under **Constant Torque Region (Low Speed)**, the motor runs constant torque, proportional to the q-axis current (i_q) and it works at maximum torque per ampere region.

At Constant Power Region (Medium to High Speed), As speed increases, back EMF rises, opposing the supply voltage. The motor produces constant power, but torque decreases with increasing speed.

At Field Weakening Region (High Speed), very high speeds, the motor enters field weakening mode by reducing the d-axis current (i_d) to limit back EMF. Torque decreases further as speed increases up to the motor speed limits, due to reduced i_q and flux.

Simulation result for Speed vs. Torque

Torque Control: The q-axis current (i_q) controls torque, while the d-axis current (i_d) influences magnetic flux.

Speed Control: Speed is controlled by adjusting the reference voltage based on rotor speed feedback, ensuring desired speed dynamics.

At medium speed, torque drops slightly while power remains constant. At maximum speed, field weakening is used to permit higher speeds, but torque decreases. In the high-speed region, torque continues to decrease as the motor arrives the field weakening mode, reducing flux and limiting power.

Power vs. Electrical Speed Characteristic Curve

At low speed, MTPA region, high torque is possible due to low back EMF. As speed increases, back EMF rises, reducing available current and torque. Power levels off or increases slowly as speed approaches maximum, and saturation arises when current and torque can no longer increase.

Magnitude Voltage vs. Electrical Speed Characteristic Curve

At low speeds or MTPA region, the back EMF is low, so less voltage is needed. As speed increases, back EMF rises, requiring more voltage to overcome resistance and

inductive effects. The voltage-speed relationship is linear in the low-speed and constant torque region. At high speeds, the voltage increases rapidly to counter the higher back EMF, and field-oriented control (FOC) is used to dynamically adjust voltage based on rotor flux and torque. This results in a less linear voltage-speed curve. Eventually, the motor reaches a maximum speed where the voltage supply can't overcome the back EMF, entering a saturation region where speed cannot increase further due to voltage limitations.

Electrical Speed verses i_q and i_d current

In IPMSM, the electrical speed vs. i_q (quadrature current) and i_d (direct current) curves are essential for understanding motor performance. These currents are controlled in field-oriented control (FOC) to regulate torque and flux. For control, i_d is typically set to zero or negative to minimize losses and prevent magnetic field weakening. Positive $i_d$values increase flux but are avoided in high-performance motors to maintain efficiency.

Control Strategy's for the currents that shows in the figure

i_q (Torque Control), i_q directly controls the torque output there for higher i_q values produce higher torque. And their **Speed vs. i_q characteristics have at** Low speed the value of i_q increases linearly to generate torque when it arrives at Medium speed the current i_q levels off or decreases as torque saturation is reached. At the last when it arrives High speed region i_q is controlled to prevent excessive torque and maintain stability.

i_d (Flux Control) the current value at Low speed, current i_d is typically zero or slightly negative. And at High speed the current i_d becomes negative to weaken rotor flux and extend speed in the field-weakening region.

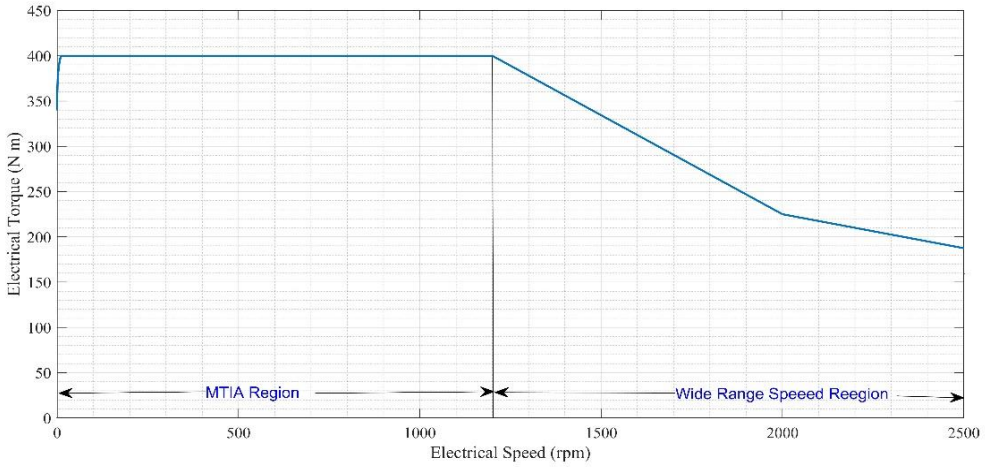

Figure 5-2: - It shows Electrical Torque vs Electrical Speed characteristics (Capability) curve of an IPMSM torque is constant at MTPA, and decreases further with speed as the motor enters wide speed range (FW region).

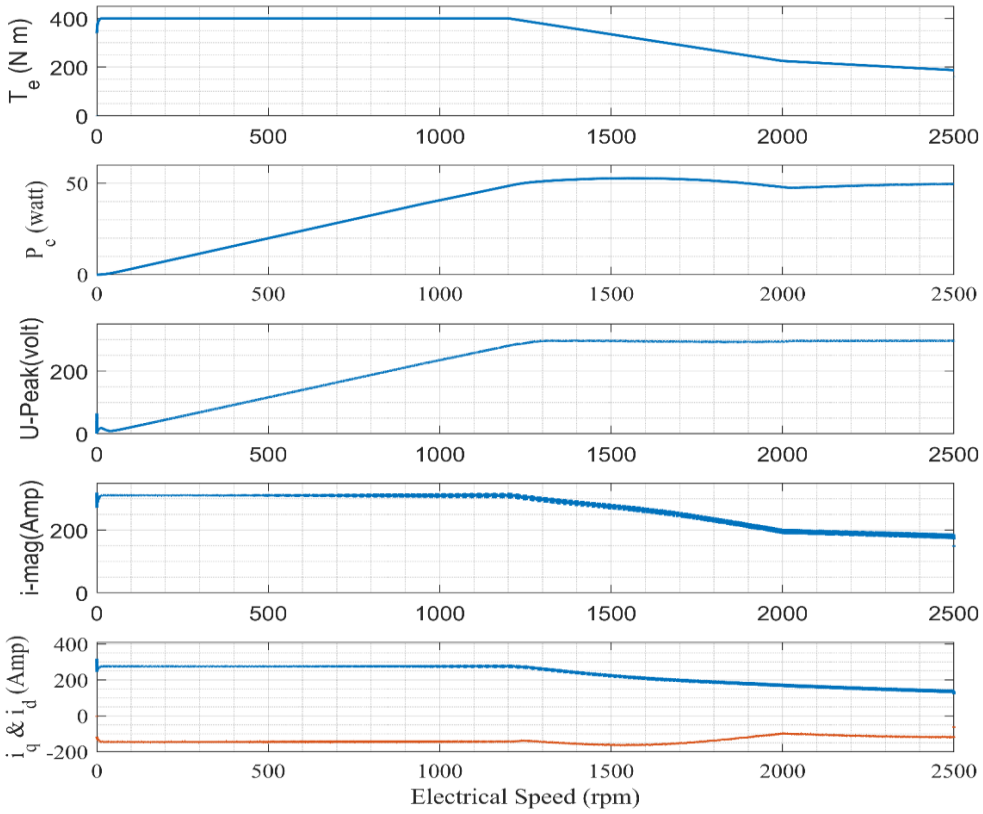

Figure 5-3: Electrical speed verses electrical Power, Magnitude voltagei_d& i_q output it shows that the behavior of their step and corves

5.1.2 Simulation and Desiccation Verification of Speed Controller Loop

The speed controller design was verified using MATLAB2022b – SIMULINK, comparing PI speed control, SMC speed control, and Integral Sliding Mode Control. In PI control, the simulation showed speed ripples when compared to the reference speed, caused by feedback issues. This often results in oscillations or instability, leading to an unstable system response. Speed and torque variations also affect acceleration and deceleration, causing ripples (overshoot) in the speed change curve.

The first test involved no load from 0 to 0.5 seconds, maximum torque (300N·m) from 0.5 to 2.5 seconds, lighter load (150N·m) from 2.5 to 5 seconds, and reverse speed from 5 to 6 seconds. The reference speed was set between 314 rpm and 628 rpm, with reversal at -314 rpm. Both steps showed overshoot in speed response when using PI control.

Simulation results using PI Speed controller and its effect

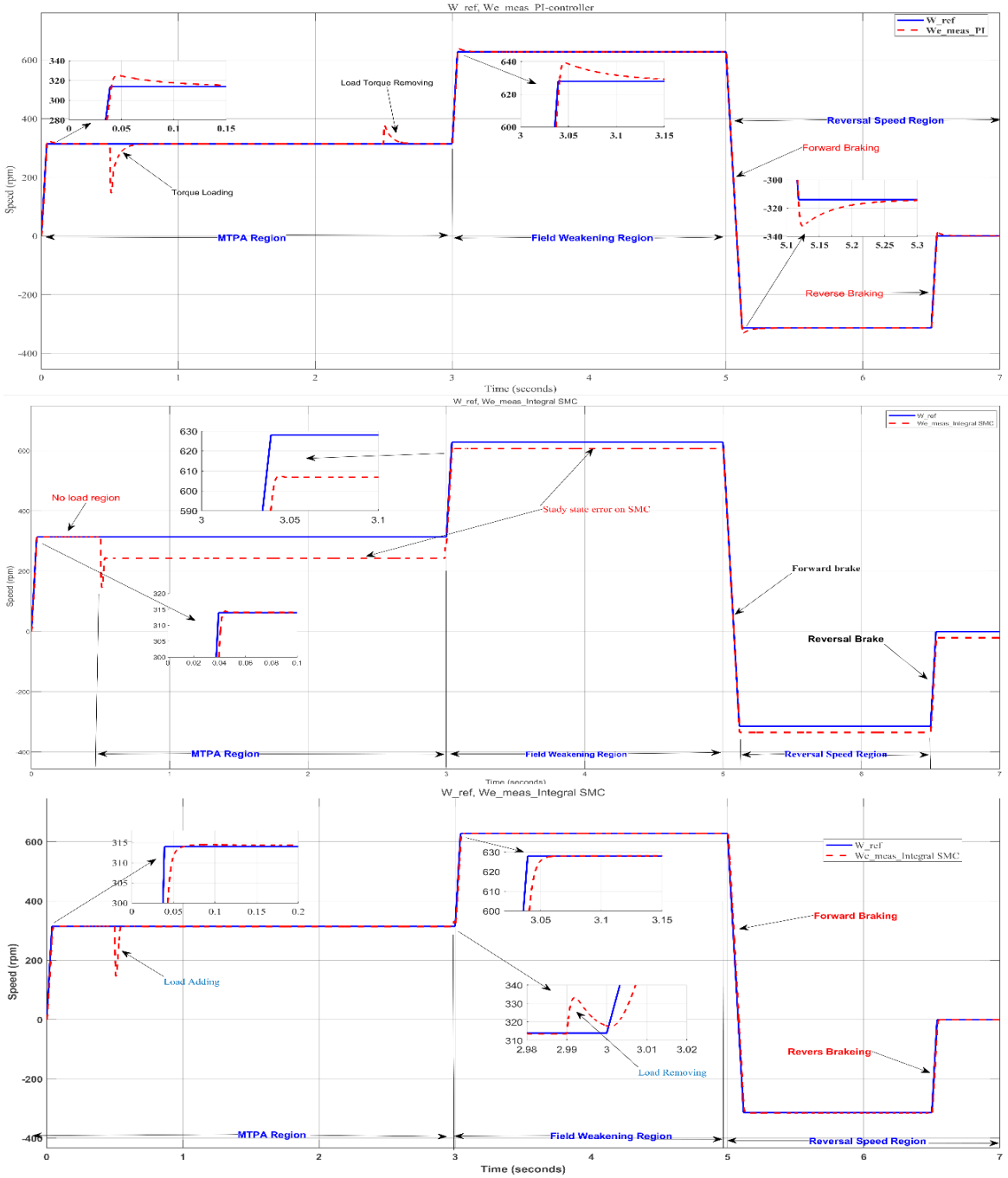

Figure 5-4: - All speed-controlled outputs (PI, SMC and I-SMC) using in deference speed from 314rpm MTPA region, 628rpm, wide speed range control and -314rpm to reversal speed

region. The blue indicates reference speed and red Brocken line is shown measured speed controlled in deference Load torque

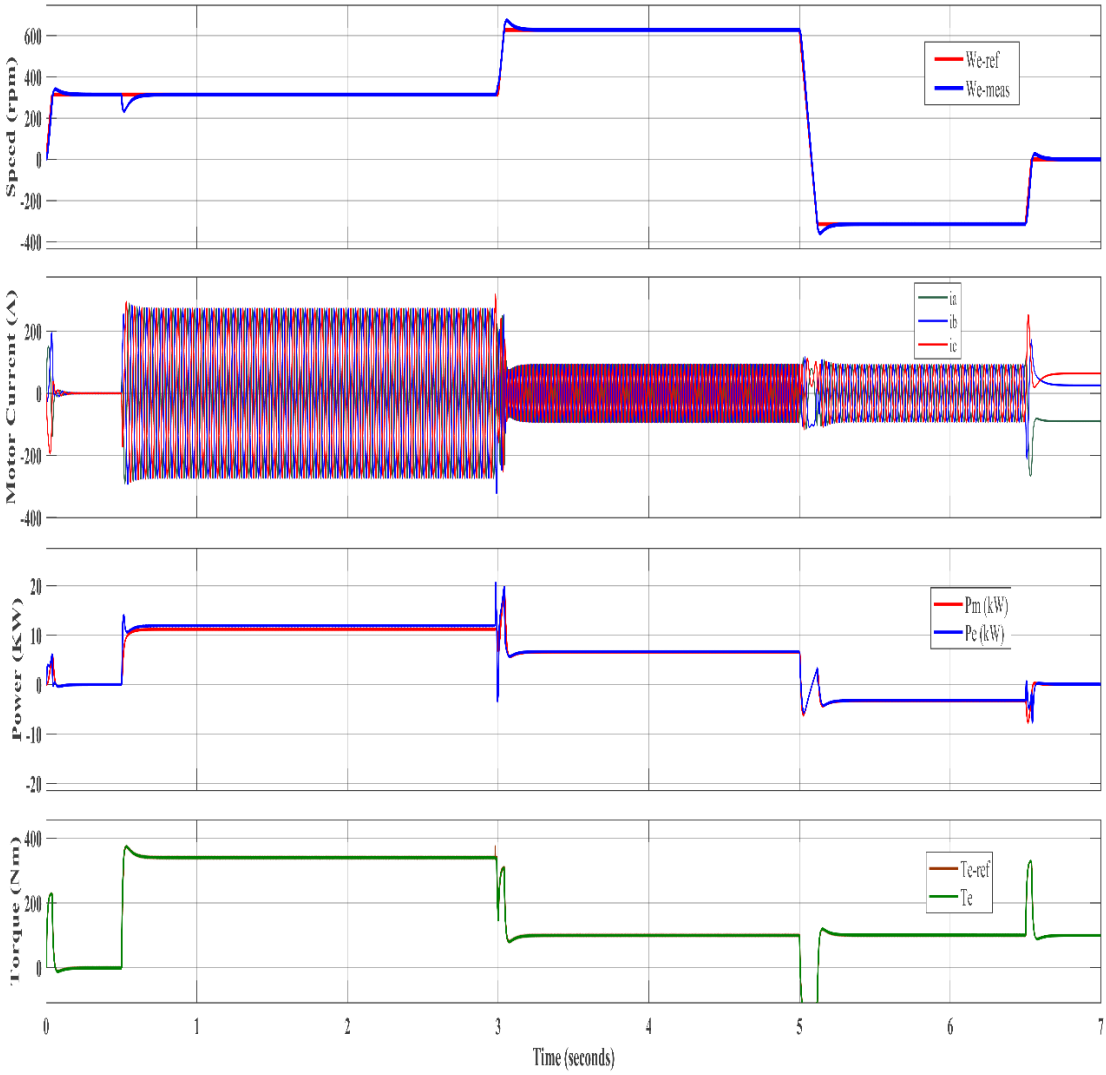

Figure 5-5: - This picture shows that three phase current output, Power out-put, Electrical torque and output speed output using PI controller

Figure 5-5 The system shows different torque and frequency oscillation states in MTPA and field weakening. In field weakening, frequency oscillations are more than three times higher than in MTPA. Power output is inversely proportional to torque, but directly proportional to speed. In the wide speed range, power increases with speed until saturation area is reached. Additionally, voltage oscillation frequency rises with both speed and power. The electrical torque output (blue line) and motor torque

output (red dashed line) vary across different torque and speed ranges when using a PI speed controller.

Simulation results using SMC Speed controller and its effect

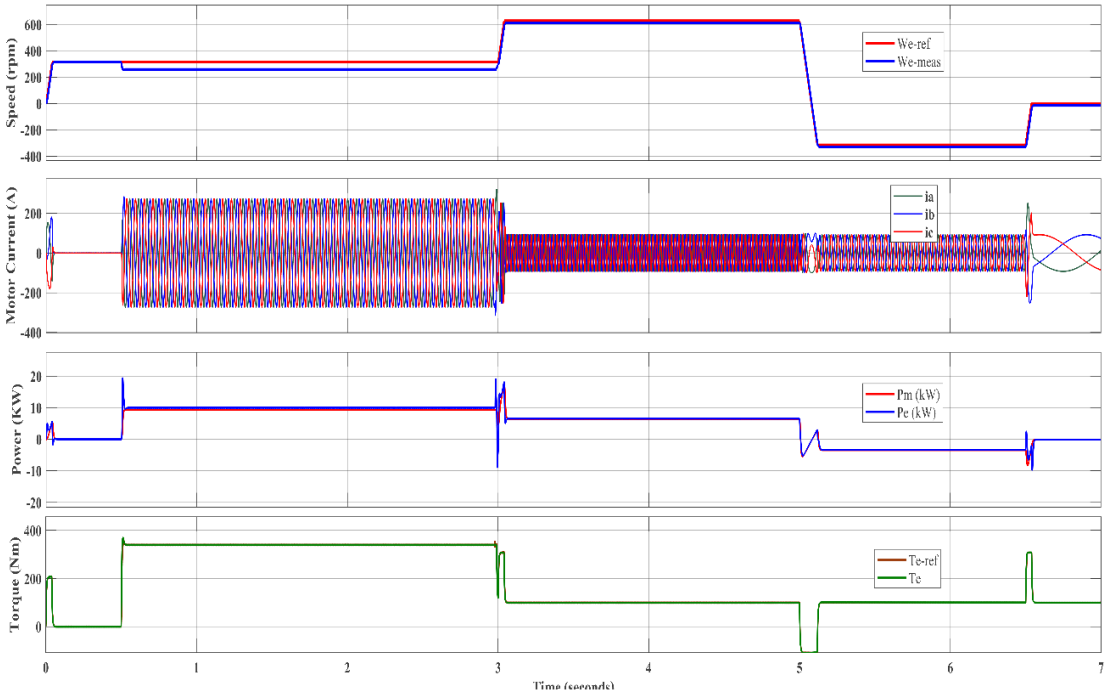

Figure 5-6: - This picture shows that three phase current output, Power out-put, Electrical torque and output speed output Using SMC controller

Integral sliding Mode controller(I-SMC) Simulation Result

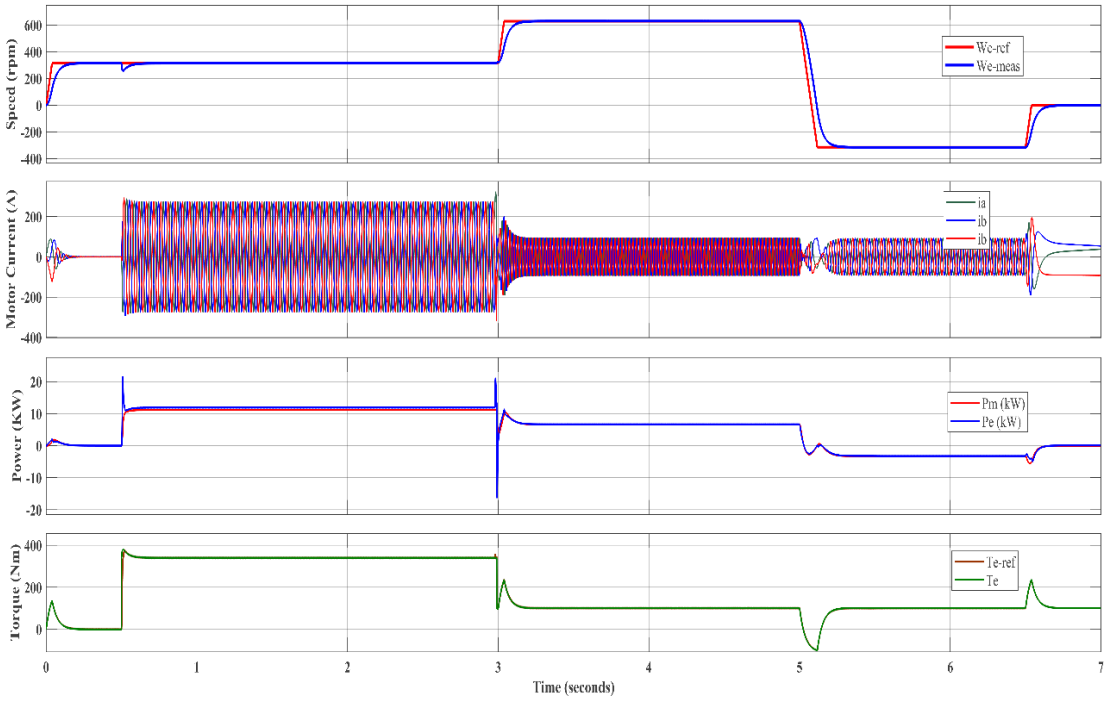

Figure 5-7: Shows that the result of three phase motor current output, Electrical Power output and electrical Torque output together using I-SMC controller.

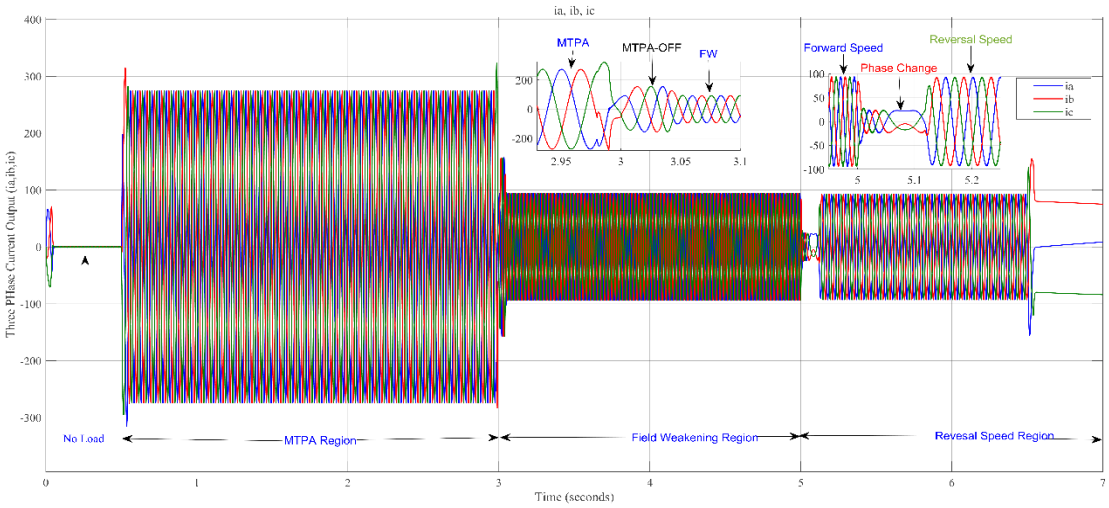

Figure 5-8: Three phase current output under MTPA and FW region

5.2 Discussion

For smooth operation of the cascade control structure, the current loop bandwidth (Bw) should be 5 to 10 times greater than the speed loop bandwidth (Bw) ($\alpha c = 5 \sim 10\ \alpha s$). The speed response using controllers designed by the SMC method shows nearly zero steady-state error and no overshoot. However, steady-state error isn't completely eliminated in this thesis due to the MTPA controller's limitations in correcting it with a sensor less speed controller. To address this, an Integral Sliding Mode Controller (I-SMC) is proposed, which eliminates steady-state error, ripple, and overshoot. Results show I-SMC offers more uniform control than PI and SMC controllers. Field-Oriented Controllers also help reduce overshoot and speed ripple during transitions between control modes.

The MTPA controller impacts motor current by increasing current, power, and torque when a load torque of 400 Nm is applied. When MTPA is switched off, motor current increases for the same torque, leading to higher stator losses. The IPMSM motor in a wide speed mode, with speeds ranging from 0 to 628 rpm, reduces torque to avoid motor saturation and inverter overload. The motor's speed and torque references should be adjusted carefully to ensure optimal performance and efficiency.

Chapter 6

6. Conclusions and Future work

6.1. Conclusions

> "The application of field weakening and Maximum Torque Per Ampere (MTPA) control techniques for an Interior Permanent Magnet Synchronous Motor (IPMSM) in speed control applications is examined in this work. The motor in question has a 550 V DC link and a 50-kW rating. MATLAB/Simulink 2022b was used to design and validate Sliding Mode Control (SMC) and Integral Sliding Mode Control (I-SMC), both of which incorporate MTPA. Strong performance was validated by simulation results, which showed efficient torque delivery over a broad speed range, especially while field weakening operation was occurring at high speeds.

MTPA, when combined with field weakening, improves motor performance, reduces stator losses, and maintains torque in a wider speed range. The control system ensures that the modulation index remains below, preventing current controller saturation. Simulation results indicated that the SMC improves motor stability, speed, and torque output compared to PI control, particularly under varying load conditions. However, a steady-state error was observed due to torque structure design. This issue was addressed with a sensor-less speed control system using second-order sliding mode or by using an I-SMC controller, which provided smoother performance and better stability.

The I-SMC controller demonstrated superior control, providing stable operation in MTPA and field weakening mode, with a smooth output and strong robustness for motor speed control in various conditions.

6.2. Future Work

For future research, work the following tasks may be considered:

For the MTPA control, it can purpose Second order sliding mode controllers to avoid electrical torque derivative output form $\frac{dT_e}{dt}$ to T_e using sensor less position estimator control. And the implemented cascaded current controller also controlled by SMC.

For the Wide Speed range Control method, it will be verified at allowable maximum torque per voltage (MTPV), reversal speed braking mechanism of the IPMSM, and regenerative braking for reuse the power, and also maximum field weakening capabilities of the IPMSM could be evaluated.

References

[1] C. Capitan, "Torque control in field weakening mode," *no. June,* vol. 84, 2009.

[2] B. Z. Y. a. H. H. Liu, "Structure-variable sliding mode control of interior permanent magnet synchronous motor in electric vehicles with improved flux-weakening method.," *{Advances in Mechanical Engineering,* vol. 10, no. SAGE Publications Sage UK: London, England, p. 1687814017704355, 2018..

[3] J. P. Desai, "13 Analytical Review of MTPA with Field Weakening Control of IPMSM on FEA Validated Design. Transactions of the Indian National Academy of Engineering.," *Transactions of the Indian National Academy of Engineering,* vol. 8, no. Springer, pp. 305-316, 2023.

[4] S. a. T. M. Hosseini, "IPMSM velocity and current control using MTPA based adaptive fractional order sliding mode controller," *Engineering science and technology, an international journal,* vol. 3, no. Elsevier, pp. 896--908, 2017.

[5] D. A. e. a. Sharma, "Enhanced mathematical modelling of interior permanent magnet synchronous machine considering saturation, cross-coupling and spatial harmonics effects. 2020 Fifteenth International Conference on Ecological Vehicles a," *2020 Fifteenth International Conference on Ecological Vehicles and Renawable Energies (EVER),* no. IEEE, 2020.

[6] M. a. G. A. a. P. F. Ezzat, "Sensorless speed control of a permanent magnet synchronous motor: high order sliding mode controller and sliding mode observer," *IFAC Proceedings Volumes,* vol. 34, no. Elsevier, pp. 1290--1295, 2010.

[7] J.-I. a. I. K. a. S. T. a. S. S.-K. Ha, "Sensorless rotor position estimation of an interior permanent-magnet motor from initial states}," *IEEE Transactions on Industry Applications,* vol. 39, no. IEEE, pp. 761--767, 2003.

[8] M. T. P. Ampere, "Field-Weakening Control (with MTPA) of PMSM".

[9] Y. a. M. Z. a. Z. X. a. C. D. a. Z. X. a. S. C. Yu, "Adaptive sliding mode backstepping control-based maximum torque per ampere control of permanent magnet-assisted synchronous reluctance motor via nonlinear disturbance observer," *Advances in*

Mechanical Engineering, p. 1687814018788750, 2018.

[10] I. a. S. V. Qureshi, “Wide speed range and torque control of ipmsm with mtpa-mtpv field weakening control,” *Arabian Journal for Science and Engineering,* no. Springer, pp. 1--16, 2023.

[11] T. a. I. {. a. {. D. a. M. J. Jer{\v{c}}i{\'c}, “Constrained field-oriented control of permanent magnet synchronous machine with field-weakening utilizing a reference governor,” *Automatika: {\v{c}}asopis za automatiku, mjerenje, elektroniku, ra{\v{c}}unarstvo i komunikacije,* vol. 58, no. KoREMA-Hrvatsko dru{\v{s}}tvo za komunikacije, ra{\v{c}}unarstvo, elektroniku, mjerenja~…, pp. 439-449, 2017.

[12] Y. MIAO, “High-accuracy torque control and estimation for interior permanent magnet synchronous machine drives with loss minimization,” *@phdthesis{miao2018high,* 2018.

[13] O. E. a. K. M. a. B. S. {\"O}z{\c{c}}iflik{\c{c}}i, “Maximum torque per ampere strategy in IPM drives for electric vehicles,” *El-Cezeri,* pp. 1405--1415, 2021.

[14] L. a. S. A. a. N. M. a. A. V. Dhamo, “Sliding-mode observer for IPMSM sensorless control by MTPA control strategy,” *IFAC-PapersOnLine,* pp. 152--157, 2016.

[15] F. a. M. S. a. M. M. Mohd Zaihidee, “Robust speed control of PMSM using sliding mode control (SMC)—A review,” *Energies,* p. 1669, 2019.

[16] S. a. K. D. R. a. L. P. a. P. S. Gambhire, “Review of sliding mode based control techniques for control system applications,” *International Journal of dynamics and control,* vol. 9, no. Springer, pp. 363--378, 2021.

[17] I. a. S. V. Qureshi, “Wide speed range and torque control of ipmsm with mtpa-mtpv field weakening control,” *Arabian Journal for Science and Engineering,* vol. 49, no. Springer, pp. 15833--15848, 2024.

[18] H. a. D. M. K. a. N. H. K. Barman, “The telecommunications divide among Indian states,” *Telecommunications Policy},* vol. 42, no. Elsevier, pp. 530--551, 2018.

[19] H. a. D. M. K. a. N. H. K. Barman, “The telecommunications divide among Indian states,” *Telecommunications Policy,* vol. 42, no. Elsevier, pp. 530--551, 2018.

[20] X. a. Z. B. a. C. D. a. Z. J. Xu, “Research on power density improvement for interior permanent magnet synchronous machine based on permanent magnet minimization,” *IET Electric Power Applications,* vol. 16, no. Wiley Online Library, pp. 1339--1351, 2022.

[21] V. C. Ilioudis, “Sensorless control of permanent magnet synchronous machine with magnetic saliency tracking based on voltage signal injection,” *Machines,* vol. 8, no. MDPI, p. 14, 2020.

[22] D. S. a. M. K. Bariša, “Comparison of maximum torque per ampere and loss minimization control for the interior permanent magnet synchronous generator,” *International Conference on Electrical Drives and Power Electronics (EDPE),* no. IEEE, pp. 497--502, . Bariša, D. Sumina and M. Kutija, "Comparison of maximum torque per ampere and loss minimization control for the interior p 2015.

[23] C. Lewin, “New Developments in commutation and Motor Control Techniques,” *Design News,* 2006.

[24] d. K. a. P. R. O. L"u, “Rotational Motion of Rigid Bodies,” *Pohl's Introduction to Physics: Volume 1: Mechanics, Acoustics and Thermodynamics,* no. Springer, pp. 91--127, 2017.

[25] M. Schweizer, “System-oriented efficiency optimization of variable speed drives,” 2012.

[26] K. M. a. R. A. D. Laundal, “Magnetic coordinate systems,” *Space Science Reviews,* vol. 206, no. Springer, pp. 27--59, 2017.

[27] W. a. J. S. a. Y. S. a. W. H. a. Z. Z. Jin, “Maximum torque per ampere control of permanent magnet reluctance hybrid rotor dual stator synchronous motor based on sliding mode speed controller,” *IET Power Electronics,* 2024.

[28] R. K. a. S. V. a. B. L. a. B. S. Sharma, Vector control of a permanent magnet synchronous motor, IEEE, 2008.

[29] R. D. a. L. T. A. a. N. D. W. Lorenz, “Motion control with induction motors,” *Proceedings of the IEEE,* vol. 82, no. IEEE, pp. 1215--1240, 1994.

[30] M. M. I. Chy, “Development and implementation of various speed controllers for wide speed range operation of IPMSM drive,” *Electric Power Systems Research,* no. @phdthesis{chy2007development, 2007.

[31] F.-J. a. H. Y.-C. a. C. J.-K. Lin, “Sensorless IPMSM drive system using saliency back-EMF-based observer with MTPA control,” *International Conference on Electrical Machines and Systems (ICEMS),* no. IEEE, pp. 3539--3545, 2014.

[32] B. a. Z. Y. a. H. H.-Z. Liu, “Structure-variable sliding mode control of interior permanent magnet synchronous motor in electric vehicles with improved flux-weakening method,” *Advances in Mechanical Engineering,* vol. 2018, no. SAGE Publications Sage UK: London, England, p. 1687814017704355}, 10.

[33] K. a. Y. T. a. Z. C. a. L. X. a. C. Y. a. L. T. a. H. J. Zhao, “Sliding mode-based velocity and torque controllers for permanent magnet synchronous motor drives system,” *The Journal of Engineering,* vol. 2019, no. Wiley Online Library, pp. 8604--8608, 2019.

[34] P. Bernard, “Study of vector control strategy on Interior Permanent Magnet

Synchronous Motors," no. bernard2023study, 2023.

[35] A. a. S. E. Hassan, "High performance direct torque control schemes for an IPMSM drive," *Electric Power Systems Research,* vol. 89, no. Elsevier, pp. 171--182, 2012.

[36] K. Ogata, Modern control engineering, 2020.

[37] R. F. a. L. T. A. Schiferl, "Power capability of salient pole permanent magnet synchronous motors in variable speed drive applications," *IEEE Transactions on Industry Applications,* vol. 26, no. IEEE, pp. 115--123, 1990.

[38] N. a. N. Y. a. H. A. M. a. Y. Y. a. Y. A. a. S. T. Urasaki, "Wide-speed range operation of interior permanent magnet synchronous motor with parameter identification," *Electric Power Components and Systems,* vol. 37, no. Taylor \& Francis, pp. 847--865, 2009.

[39] K. A. M. S. D. J. N. a. W. X. Zhou, "Zhou, K., Ai, M., Sun, D., Field weakening operation control strategies of PMSM based on feedback linearization. Energies, 12(23), p.4526.," *Energies,* vol. 12, no. MDPI, p. 4526., 2019.

[40] F. a. D. R. Rahman, "Control of Interior Permanent Magnet Synchronous Machines," *AC Electric Motors Control: Advanced Design Techniques and Applications,* no. iley Online Library, pp. 398-428., 2013.

[41] Y. a. W. X. a. X. W. a. D. M. Wang, "Full-speed range encoderless control for salient-pole PMSM with a novel full-order SMO}," *Energies},* vol. 11, no. MDPI, p. 2423, 2018.

[42] K. a. A. M. H. a. D. T. D. Suleimenov, Integral sliding mode controller design for permanent magnet synchronous machines, 2019 International Conference on System Science and Engineering (ICSSE) ed., IEEE, 2019.

[43] F.-J. a. L. Y.-H. a. L. J.-R. a. L. W.-T. Lin, "Interior permanent magnet synchronous motor drive system with machine learning-based maximum torque per ampere and flux-weakening control," *Energies,* vol. 14, no. MDIP, p. 346, 2021.

[44] S. P. K. K. D. a. L. G. Kim, "Kim, S., Park, K., High-Performance Permanent Magnet Synchronous Motor Control With Electrical Angle Delayed Component Compensation.," *IEEE Access,* vol. 11, no. IEEE, pp. 129467--129478, 2023.

[45] W. a. J. S. a. Y. S. a. W. H. a. Z. Z. Jin, "Maximum torque per ampere control of permanent magnet reluctance hybrid rotor dual stator synchronous motor based on sliding mode speed controller," *IET Power Electronics,* no. Wiley Online Library, 2024.

[46] J. a. W. J. a. Y. B. Chen, "Simulation Research on Deadbeat Direct Torque and Flux Control of Permanent Magnet Synchronous Motor," *Simulation Research on Deadbeat Direct Torque and Flux Control of Permanent Magnet Synchronous Motor,* vol. 15, no.

MDPI, p. 3009, 2022.

[47] Y. M. Z. Z. X. C. D. Z. X. a. S. C. Yu, “Yu, Y., Mi, Z. Adaptive sliding mode backstepping control-based maximum torque per ampere control of permanent magnet-assisted synchronous reluctance motor via nonlinear disturbance observer.,” *Advances in Mechanical Engineering,* p. 1687814018788750, 2018.

[48]

[49] M. S. Zaky, “Robust sliding mode speed controller-based model reference adaptive system (MRAS) and load torque estimator for Interior permanent magnet synchronous motor (IPMSM) drives,” *Electric Power Components and Systems,* vol. 43, no. Taylor \& Francis, pp. 1523--1533}, 2015.

[50] T. a. I. {. a. {. D. a. M. J. Jer{\v{c}}i{\'c}, “Constrained field-oriented control of permanent magnet synchronous machine with field-weakening utilizing a reference governor,” *Automatika: {\v{c}}asopis za automatiku, mjerenje, elektroniku, ra{\v{c}}unarstvo i komunikacije,* vol. 58, no. KoREMA-Hrvatsko dru{\v{s}}tvo za komunikacije, ra{\v{c}}unarstvo, elektroniku, mjerenja~…, pp. 439--449, 2017.

[51] I. a. R. M. N. a. F. L. M. a. F. N. a. L. R. a. O. M. Schapiro, “The ultrafast photoisomerizations of rhodopsin and bathorhodopsin are modulated by bond length alternation and HOOP driven electronic effects,” *Journal of the American Chemical Society,* vol. 133, no. ACS Publications, pp. 3354--3364, 2011.

[52] S.-H. a. J. T. M. a. S. W. L. Han, “Torque ripple reduction in interior permanent magnet synchronous machines using the principle of mutual harmonics exclusion,” *2007 IEEE Industry Applications Annual Meeting,* no. IEEE, pp. 558--565, 2007.

[53] Y. Ogata, “Increased probability of large earthquakes near aftershock regions with relative quiescence,” *Journal of Geophysical Research: Solid Earth,* vol. 106, no. Wiley Online Library, pp. 8729--8744, 2001.

Appendix

Initialization file

```
%PI_gain for tunning q-axis
%zeta1 = 0.98432;
%gamma1 = 0.8631;
%SMC_gain
zeta1 =.432;
gamma1 = 0.6802;
Wnq = (1/(1-gamma1))*(Rs/Lq);
kcq = (2*zeta1*Wnq*Lq)-Rs;
t_iq = (2*zeta1*Wnq*Lq-Rs)/((Wnq^2)*Lq);
%%
%PI_gain for tunning d-axis
zeta2 = 0.06;
gamma2 = 0.047;
%SMC_gain
%zeta2 = 0.6;
%gamma2 = 0.47;
Wnd = (1/(1-gamma2))*(Rs/Ld);
kcd = (2*zeta2*Wnd*Ld)-Rs;
t_id = (2*zeta2*Wnd*Ld-Rs)/((Wnd^2)*Ld);
%%
%zeta3 = 0.2; % zeta1
%PI_gain for tunning speed gain
gamma3 = 0.322;
Wns=(1/(1-gamma3))*(B/J);
kcs=(2*zeta1*Wns-(B/J))/((0.75 * (P^2))*((Lambda_m)+(Ld-Lq))/J);
t_is =(2*zeta1*Wns-(B/J))/(Wns^2);


%% Parameters file for SPS model: InteriorPMSMFieldOrientedControl.slx
VSP = [1200,2000,3000,4000,5000,6000];
tsp = [0,2.0,4.0,6.0,8.0,10.0];
%% SPS sample time (s)
Ts=1e-5;
%
%% Motor parameters
%ntro
Tnom = 400;        % Nominal torque                 (N.m)
wnom = 1200; %400;%1200;       % Nominal motor speed            (rpm)
wmax = 6000; %1200;%6000;       % Maximum motor speed            (rpm)
Ld = 1.597e-3;     % Stator d-axis inductance       (H)
Lq = 2.057e-3;     % Stator q-axis inductance       (H)
Rs = 6.5e-3;       % Stator resistance per phase    (Ohm)
lambda = 0.1757;   % Permanent magnet flux linkage  (V.s)
p = 4;             % Number of pole pairs
J = 0.09;          % Rotor inertia                  (Kg.m^2)
F = 0.002;         % Friction coefficient           (N.m.s)
Vdc_nom = 550;     % Nominal DC voltage (V)
%
%% Control parameters
%
% Speed regulator
```

```
Kp_wreg= 1.5; %4.5; %3.5;        % Proportional gain
Ki_wreg= 50; %90;  %70;         % Integral gain
Limit_wreg=Tnom;      % Regulator output limit
%
% Torque Limiter
rpm_data= [0   1200 2000 3000 4000 5000 6000]; % Speed (rpm)
Tmax_data=[400 400  225  150  100  80   70  ]; % Torque(N.m)
%
% Current regulator
Kp_Ireg= 0.3; %1.2;  %2.4;                % Proportional gain
Ki_Ireg= 0.50; %20; %40;                 % Integral gain
Limit_Ireg=Vdc_nom/sqrt(3);  % Regulator output limit
%
Fsw=2000;                    % SVPWM switching frequency (Hz)
%
%%
%SMC  gain
alpha = 0.160750;
beta = 0.015;
C = 11.955;
K =50.1;


k=1;
for is=0:0.1:Isn
p=[2 Psi_m/(Ld-Lq) -is*is];
R=roots(p);
if(R(1)<R(2)), id=R(1);
else
id=R(2);
end
iq1=sqrt(is*is-id*id);
Te1=1.5*pb*(Psi_m+(Ld-Lq)*id)*iq1;
Uid(k)=id;
Uiq1(k)=iq1;
UTe1(k)=Te1;
i=is;
k=k+1;
end
M1=[UTe1;Uid];
M21=[UTe1;Uiq1];
plot(Uid,UTe1,'-',Uiq1,UTe1,'-r')
```

SIMULINK® Blocks

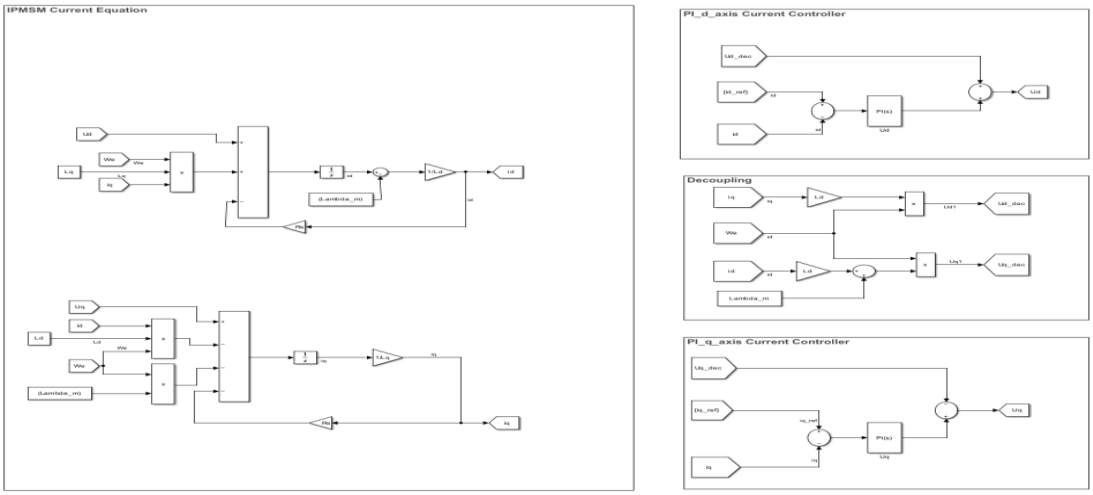

Figure I: shows that the measured PI-controller on dq frame

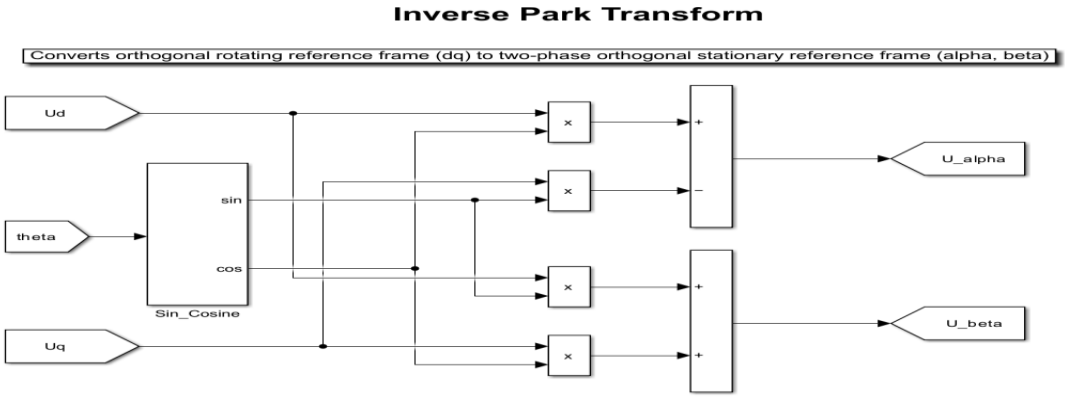

Figure II: Shows that Invers park transformation convert orthogonal reference dq frame.

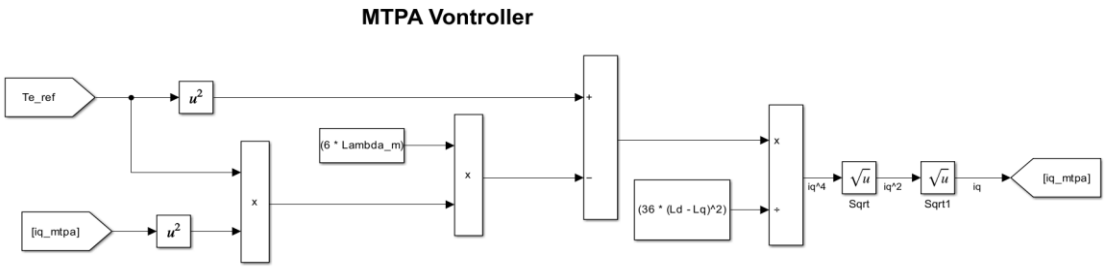

Figure III: shows that MTPA controller block diagram

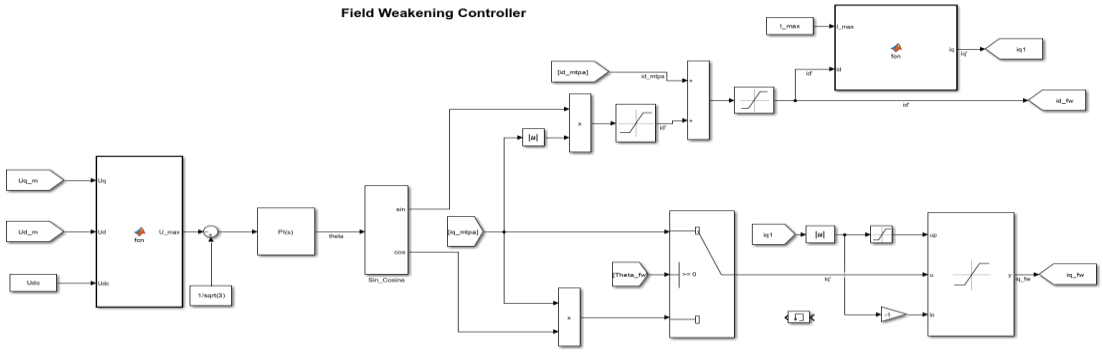

Figure IV: Wide range speed controller for field weakening with modulation index

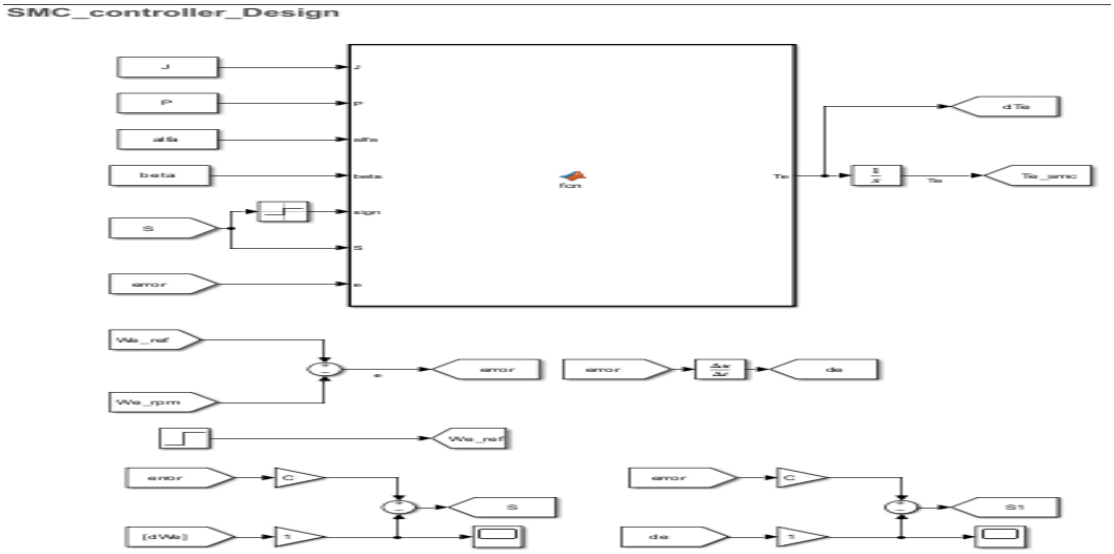

Figure V: shows that SMC controller using MATLAB functional block

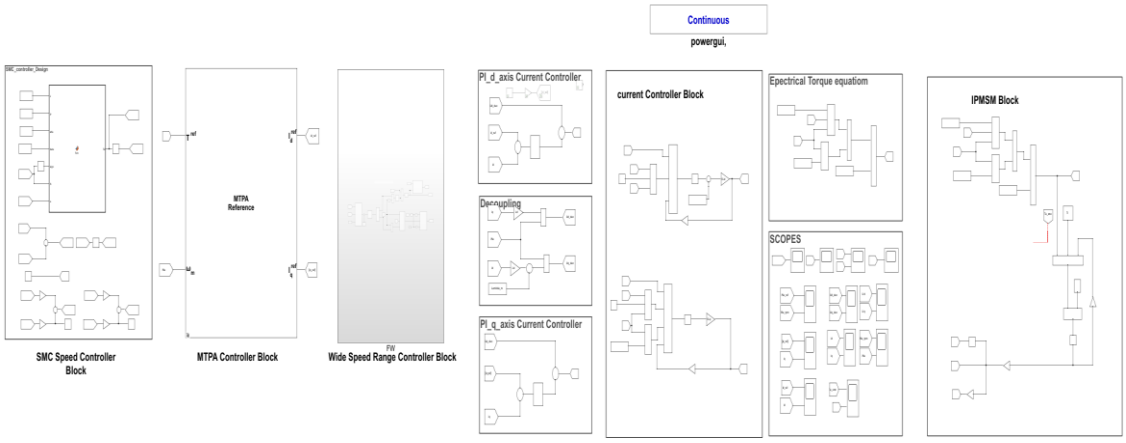

Figure VI: shows all controlling mechanism MTPA and wide range speed controller block diagram without SVPWM and Invertor

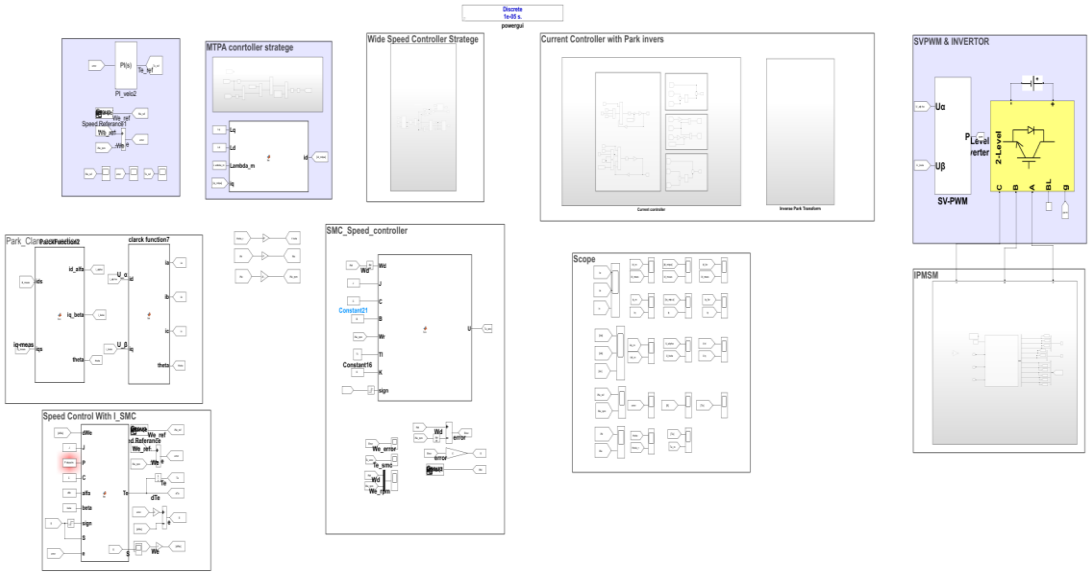

Figure VII: shows all controlling mechanism MTPA and wide range speed controller block diagram using SVPWM and Invertor

Sliding Mode Based Maximum Torque per Ampere and wide speed range Control for Interior Permanent Magnet Synchronous Motor Drive